SINTEF

OC2018 F-073-WP2 - Restricted

Report

LFCS
Large Floating Coastal Structures

LFCS Review report – Environmental loads

Methods for the estimation of loads on large floating bridges

Author(s)
Nuno Fonseca
Erin Bachynski

SINTEF Ocean AS
Ships and Offshore Structures
2018-11-16

SINTEF Ocean AS
Address:
Postboks 4762 Sluppen
NO-7465 Trondheim
NORWAY
Switchboard: +47 464 15 000
ocean@sintef.no
www.sintef.no/ocean
Enterprise /VAT No:
NO 937 357 370 MVA

Report

LFCS Review report – Environmental loads

Methods for the estimation of loads on large floating bridges

REPORT NO.	VERSION	DATE
OC2018 F-073-WP2	4.0	2018-11-16

KEYWORDS:
wind loads; wave loads; current loads; large floating bridges;

AUTHOR(S)
Nuno Fonseca
Erin Bachynski

CLIENT(S)
KPN-project LFCS Industry partners and Norwegian Research Council (NRC)

CLIENT'S REF.	NUMBER OF PAGES/APPENDICES:
[Clients ref]	41

CLASSIFICATION	CLASSIFICATION THIS PAGE	ISBN
Restricted	Restricted	

ABSTRACT

The document presents a review of state-of-the-art methods to calculate environmental loads on large floating bridges. It is a deliverable from WP2 of the Design and verification of Large Floating Costal Structures (LFCS) KPN project.

The environmental loads arise from wind, waves and current actions. The report starts with a review of physical effects contributing to the loads and methods used to calculate them. Regarding wind loads, most knowledge comes from the large bridge engineering field, while methods for wave and current loads are developed for the offshore oil and gas sector for more than 40 years. Use of the existing methods for floating bridges is discussed.

The second part of the report reviews the methods applied for the Bjørnafjorden designs, starting with the Statens vegvesen Design Basis and continuing with the actual feasibility studies for the straight bridge and curved bridge solutions.

The report ends with identification of gaps on the calculation methods and recommendations for further studies.

PREPARED BY	CHECKED BY	APPROVED BY
Nuno Fonseca / Erin Bachynski	Halvor Lie	Vegard Aksnes

Document history

VERSION	DATE	VERSION DESCRIPTION
1.0	2018-09-17	Draft version
2.0	2018-09-17	Draft version with additional text in Sections 1, 5 and 6.
3.0	2018-09-17	Draft version after internal review
4.0	2018-11-16	Final

SINTEF

Table of contents

1. Summary

The document presents a review of the state-of-the-art methods to calculate environmental loads on large floating bridges. The loads arise from wind, waves and current actions. The report starts with a review of physical effects contributing to the loads and methods used to calculate them. Regarding wind loads, most knowledge comes from the large bridge engineering field, while methods for wave and current loads are developed for the offshore oil and gas sector for more than 40 years. Use of existing methods for floating bridges is discussed.

The second part of the report reviews the methods applied for the Bjørnafjorden designs, starting with the Design Basis (Statens vegvesen / NPRA) and continuing with the actual feasibility studies for the straight bridge and curved bridge solutions. The report ends with identification of gaps on the calculation methods and recommendations for further studies.

The Bjørnafjorden design analyses and feasibility studies consulted for this report represent very good achievements, where advanced methods from bridge engineering design are combined with hydrodynamic methods from the oil and gas sector. These analyses truly represent the state-of-the-art in terms of methods for a complete design analysis of large floating bridges.

The present report identifies is a list of items, or gaps, related to calculation of environmental load components where simplifications have been introduced, compared to the state-of-the-art methods. The simplifications are introduced to keep the global methodology and effort at a manageable level. These simplifications may either introduce uncertainties on the predictions, or they may be acceptable, but that is not documented. There are also a couple of challenges which are beyond today's calculation methods possibilities.

Table 1 lists the identified gaps and recommended studies.

The report recommends that all gaps are addressed during the LFCS KPN project. However, for several of the gaps, only simplified studies, or discussions, are recommended, aiming at achieving a better understanding of the effects on the global analysis predictions. A few gaps are selected for more complete developments or studies.

Most of the proposed studies assume a functional SIMA/SIMO/RIFLEX numerical model for the case study floating bridge will be available.

Model test data is expected to provide important information, both for physical insight and for validation of numerical approaches and simplifications. Ideally, the test program of WP5 should also take into consideration the studies recommended herein.

Table 1 : List of identified gaps and recommendations for further studies (more details in Sections 6 and 7).

Gap	Recommended study/development
Frequency-dependent wind loads	Implement FDAC load formulation in SIMO-RIFLEX (possibly only through SIMO DLL formulation for initial application)
NQSA vs. FDAC vs. NA+dynamic stall model	Compare several aerodynamic load formulations in order to see if NA+dynamic stall can represent effects from FDAC, and in order to compare the damping obtained from different load models.
Flutter dependence on large horizontal motions	(Out of scope of present work)

Inhomogeneous wave loads	Generalize SIMA/SIMO to handle different environments for different pontoons
Inhomogeneous wave loads	Investigate the effects of neglecting wave inhomogeneity on the diffraction solution
Multi-body interactions	Assess importance of multi-body hydrodynamic interactions between floaters on the WF and LF responses
Viscous effects	Assessment of viscous effects generated by the floater, on the WF and on the LF responses
WF motion and wave drift	Assessment of WF motions effects on the estimation of wave drift forces and on LF bridge responses
Wave-current and wave drift	Assessment of wave-current interactions on the wave drift forces and on the LF bridge responses
Wave drift damping	Assessment of wave drift damping effects on the LF bridge responses
Wave directionality and wave drift	Discussion on the effects of short crested vs long crested waves on the calculation of LF responses
Wave directionality and wave drift	Discussion on superposition principle to calculate wave drift forces from wind waves and swell from different directions
Full QTF vs Newman's	Simple assessment of full QTF vs Newman's approximation for one floater
Finite water depth	Discuss the consequences of neglecting finite water depth effects on the calculation of WF and LF responses

2. Introduction

The KPN project "Design and verification of Large Floating Coastal Structures" (LFCS) started with a kick-of Nov.30, 2017, with a planned duration to summer of 2021. The project was established by SINTEF Ocean and NTNU with the support of the Norwegian Research Council, the Norwegian Public Road Administration, Hydro ASA, Multiconsult AS, SWECO AS, and LMG Marin AS

Compared with well-established methods in ocean engineering, the following critical issues are initially identified for the analysis of large floating coastal structures,

- varying bathymetry and inhomogeneous environmental conditions over the extension of the structure
- inhomogeneous environmental loads over the structure,
- hydroelasticity of large floating coastal structures under inhomogeneous conditions,
- mooring and station-keeping of large flexible floating structures,
- modelling of hydroelastic effects in combinations with articulated/elastic interconnections between structural parts.

One objective of the present project is to improve the understanding of each of these separate topics, and then to provide input to a consistent procedure for design and verification of large floating coastal structures. The project is then organized in work packages according to the identified topics above:

- WP1 - Environmental description
- WP2 - Environmental loads
- WP3 - Structural response
- WP4 - Mooring and positioning
- WP5 - Model testing

In addition, the LFCS administrative tasks have been organized in a work package WP0.

Review phase:

The first phase of the project is devoted to a review of work already performed for relevant existing structures, for conceptual studies performed for potential crossings as well as additional work on measurements, modelling, simulations related to coastal areas which in all comprises the state of the art. This also included a 2-day workshop on March 7-8 with emphasis on environmental description, modelling and loads, and structural response based on presentations from the LFCS industry partners and specially invited external presenters.

This document describes and summarizes the review work performed for Work Package 2 (WP2) – Environmental loads, identifying gaps and uncertainties recommended for further study.

3. State of the art review

3.1 Wind loads

The state-of-the-art wind load models for bridges in general are assumed to apply to floating bridges as well. The most important of these loads are typically the loads on the girder, which are often (Jain, Jones, & Scanlan, 1996; Strømmen, 2006) divided into

- Steady components,
- Aeroelastic (motion-dependent) components,
- Buffeting (motion-independent) components.

Note that vortex shedding effects are not addressed specifically in this review: we assume that the designs have been checked to avoid vortex-induced resonances. According to Strømmen (2006), "vortex shedding effects will usually occur at fairly low mean wind velocities, buffeting will usually be the dominant effect in an intermediate velocity region, while at high wind velocities motion-induced load effects may entirely govern the response." Two main methods for computing the aerodynamic loads are used in the industry today: nonlinear quasi-static airfoil theory, or frequency-dependent flutter derivatives. These methods account for the buffeting and aeroelastic loads in different manners and are described in greater detail in Sections 3.1.1 and 3.1.2. More advanced methods, which are encountered in the state-of-the-art research but have not been seen in the industry studies so far, are summarized briefly in 3.1.3.

3.1.1 Nonlinear quasi-static airfoil theory (NQSA)

According to nonlinear quasi-static airfoil theory, the total loads on the bridge girder can be found based on the relative velocity (V_{rel}, between the girder and incoming wind) and known lift, drag, and moment coefficients as a function of the instantaneous angle of attack (α). This formulation gives the total aerodynamic load on the girder section in a convenient manner for time domain analysis.

$$\boldsymbol{q_{tot}} = \frac{1}{2}\rho V_{rel}^2 \begin{bmatrix} \cos\beta & -\sin\beta & 0 \\ \sin\beta & \cos\beta & 0 \\ 0 & 0 & 1 \end{bmatrix} \begin{bmatrix} DC_D(\alpha) \\ BC_L(\alpha) \\ B^2 C_M(\alpha) \end{bmatrix}$$

The angle β refers to the angle between the relative wind velocity and the global coordinate system, while the dimensions D and B refer to cross-sectional dimensions of the girder, as shown in Figure 1.

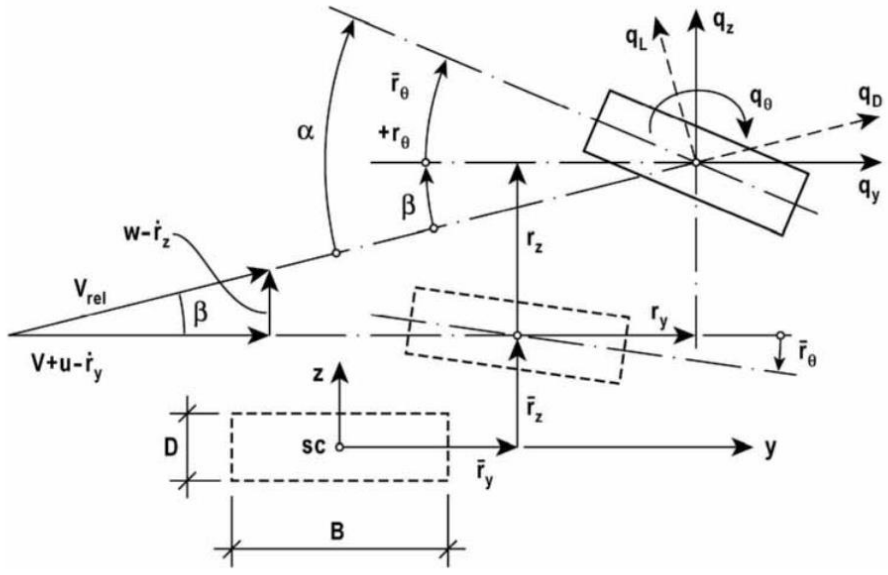

Figure 1: Coordinate systems. Figure from (Strømmen, 2006).

This type of formulation is already available in SIMA (in both SIMO and RIFLEX) and has been used in analyses of the Bjørnafjorden floating bridge designs. There is no frequency-dependence in this type of model, and the coefficients can be obtained from literature, CFD, or from experiments.

3.1.2 Frequency-dependent aerodynamic coefficients (FDAC)

Following (Strømmen, 2006), by linearizing the formulation in 3.1.1 (assuming that the turbulent wind velocities and the motions of the girder are small), one can obtain an expression of the form:

$\boldsymbol{q_{tot}} = \boldsymbol{q} + \boldsymbol{B_q v} + \boldsymbol{C_{ae}\dot{r}} + \boldsymbol{K_{ae} r}$.

The fluctuating wind velocities are denoted $\boldsymbol{v}$, and the displacements of the girder section are contained in $\boldsymbol{r}$.

$$\boldsymbol{v} = \begin{bmatrix} u \\ w \end{bmatrix}$$

$$\boldsymbol{r} = \begin{bmatrix} r_y \\ r_z \\ r_\theta \end{bmatrix}$$

The mean part of the load is obtained based on the drag, lift, and moment coefficients evaluated at the mean angle of attack $\bar{\alpha} = \overline{r_\theta}$.

$$\bar{\boldsymbol{q}} = \frac{\rho V^2 B}{2} \begin{bmatrix} \left(\frac{D}{B}\right)\overline{C_D} \\ \overline{C_L} \\ B\overline{C_M} \end{bmatrix}$$

The dynamic loading due to the turbulent variations in the wind speed (i.e. the buffeting component) is captured by $\boldsymbol{B_q v}$, where

$$\boldsymbol{B_q} = \frac{\rho B V}{2} \begin{bmatrix} 2\left(\frac{D}{B}\right)\bar{C}_D & \left(\left(\frac{D}{B}\right)C_D' - \bar{C}_L\right) \\ 2\bar{C}_L & \left(C_L' + \left(\frac{D}{B}\right)\bar{C}_D\right) \\ 2B\bar{C}_M & BC_M' \end{bmatrix}$$

The dynamic loading due to the motions of the girder section is divided into a component proportional to the velocity ($\boldsymbol{C_{ae}\dot{r}}$) and a component proportional to the displacement ($\boldsymbol{K_{ae} r}$).

$$\boldsymbol{C_{ae}} = -\frac{\rho V B}{2} \begin{bmatrix} 2\left(\frac{D}{B}\right)\bar{C}_D & \left(\left(\frac{D}{B}\right)C_D' - \bar{C}_L\right) & 0 \\ 2\bar{C}_L & \left(C_L' + \left(\frac{D}{B}\right)\bar{C}_D\right) & 0 \\ 2B\bar{C}_M & BC_M' & 0 \end{bmatrix}$$

$$\boldsymbol{K_{ae}} = \frac{\rho V^2 B}{2} \begin{bmatrix} 0 & 0 & \left(\frac{D}{B}\right)C_D' \\ 0 & 0 & C_L' \\ 0 & 0 & BC_M' \end{bmatrix}$$

This formulation is extended by allowing for frequency-dependence in the aerodynamic coefficients and their derivatives, and the matrices are usually written in terms of the so-called aerodynamic derivatives. The matrices are further normalized with respect to the natural frequency ω_i of the i-th mode shape for which the coefficients were determined. This natural frequency depends on the mean wind speed and is thus denoted as $\omega_i(V)$.

$$\boldsymbol{C_{ae}} = \frac{\rho B^2}{2}\omega_i(V)\begin{bmatrix} P_1^* & P_5^* & BP_2^* \\ H_5^* & H_1^* & BH_2^* \\ BA_5^* & BA_1^* & B^2A_2^* \end{bmatrix}$$

$$\boldsymbol{K_{ae}} = \frac{\rho B^2}{2}\omega_i(V)\begin{bmatrix} P_4^* & P_6^* & BP_3^* \\ H_6^* & H_4^* & BH_3^* \\ BA_6^* & BA_4^* & B^2A_3^* \end{bmatrix}$$

The 18 aerodynamic derivatives (P_i^*, H_i^*, A_i^*) are defined below.

$$\begin{bmatrix} P_1^* & H_1^* & A_1^* \\ P_2^* & H_2^* & A_2^* \\ P_3^* & H_3^* & A_3^* \\ P_4^* & H_4^* & A_4^* \\ P_5^* & H_5^* & A_5^* \\ P_6^* & H_6^* & A_6^* \end{bmatrix} = \begin{bmatrix} -2\bar{C}_D\frac{D}{B}\frac{V}{B\omega_i(V)} & -(C_L' + \bar{C}_D\frac{D}{B})\frac{V}{B\omega_i(V)} & -C_M'\frac{V}{B\omega_i(V)} \\ 0 & 0 & 0 \\ C_D'\frac{D}{B}\left(\frac{V}{B\omega_i(V)}\right)^2 & C_L'\left(\frac{V}{B\omega_i(V)}\right)^2 & C_M'\left(\frac{V}{B\omega_i(V)}\right)^2 \\ 0 & 0 & 0 \\ \left(\bar{C}_L - C_D'\frac{D}{B}\right)\frac{V}{B\omega_i(V)} & -2\bar{C}_L\frac{V}{B\omega_i(V)} & -2\bar{C}_M\frac{V}{B\omega_i(V)} \\ 0 & 0 & 0 \end{bmatrix}$$

An example of these coefficients (for the Hardanger bridge) is shown in Figure 2.

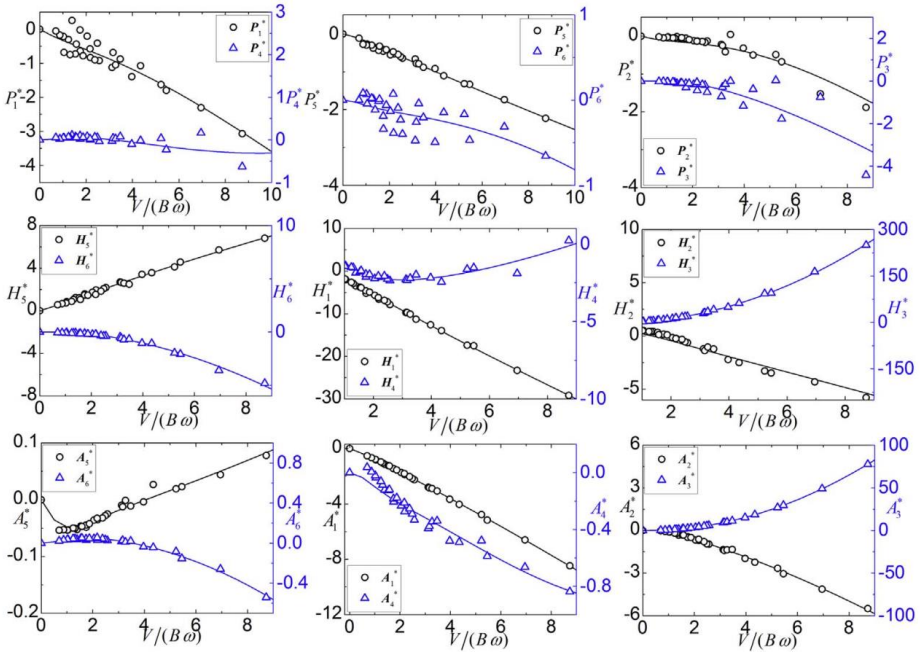

Figure 2: Aerodynamic derivatives for the Hardanger bridge from (Xu, Øiseth, & Moan, 2018).

This type of formulation can be implemented through a state-space type of formulation or through a convolution integral. The aerodynamic derivatives approach enables detection of flutter or galloping. In order to use this formulation, however, one needs the frequency-dependent aerodynamic derivatives as input. These derivatives are typically derived experimentally and may not be available at the early design stage, although one may be able to find results for similar sections.

3.1.3 Dynamic corrections to the nonlinear quasi-static airfoil theory

The NQSA approach can only capture the static relationship between the angle of attack and the aerodynamic lift, drag, and moment. This approach, which neglects any fluid memory, is considered to be fairly accurate for reduced velocity $U_r = \frac{V}{nB}$ greater than approximately 10 (Carassale, 2014), where n is the oscillating frequency of the bridge deck.

Several different approaches have been considered for including memory effects in combination with a nonlinear load formulation. Corrections in the QS theory to account for the dependence on reduced wind velocity were first considered in the 1990's (Diana G. B., 1993). The approach was later extended to a rheological model which takes the dynamic angle of attack as input and uses a combination of nonlinear springs and dashpots to calculate the resulting aerodynamic force (Diana G. R., 2006). An example of the lift forces for a pitching bridge section under different flow conditions is shown in Figure 3. In a quasi-static approach, the lift coefficient would be single-valued for a given angle of attack. The rheological approach has some similarities to the dynamic stall approaches used for wind turbines. Other approaches using, for example, Volterra frequency-response functions have also been developed for including nonlinearities and frequency-dependence simultaneously (Carassale, 2014).

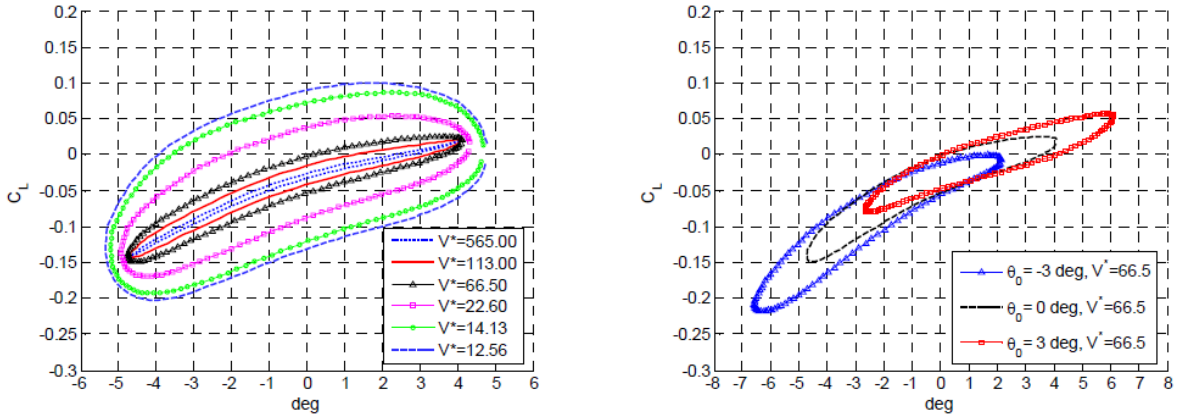

Figure 3: Hysteresis cycle in the lift force for different combinations of reduced velocity and mean angle of attack. (Diana G. R., 2006)

3.2 Wave and current loads

3.2.1 Introduction

Floaters of large floating bridges may respond to wave and current actions with motions at three different frequency regimes, namely: low frequency motions (LF), wave frequency motions (WF) and high frequency motions (HF).

LF motions are induced by second order wave drift forces, or slowly varying wave drift forces. There are interactions with the current velocity, therefore wave drift forces depend on the current. LF response on floating bridges may occur for the horizontal modes of motion perpendicular to the bridge girder.

WF forces occur at the wave frequency, they are the largest force components and induce the WF motions. Typically, floating moored structures are designed such that the natural frequencies are outside the wave frequency range. Such solution might not be possible, or advantageous, for large floating bridges, which are characterized by many natural frequencies spanning along a wide range.

Wave and current loads are not expected to induce HF motion responses of the bridge, except, possibly, in case the floating foundations are anchored to the seabed by tensioned legs. Tensioned leg moorings are not considered in this report.

In addition to dynamic motion responses, wave and current mean loads will result in mean motion offset of the bridge, mainly in the horizontal plane. In this respect, it is relevant to note that the current loads can be separated in two components. The first is the load due to steady current alone (no waves). The second component is related to the interaction between waves and current, which affects the mean, the WF and the LF wave loads.

3.2.2 Loads from steady current

Current will mainly induce a steady force on the floaters. Depending on the hull geometry, current may also induce vortex induced oscillating forces, which are discussed further ahead. Although the force will have components in all six directions of a Cartesian coordinate system, in general only the horizontal components will be relevant and especially in the direction perpendicular to the bridge girder. Current loads are given by a combination of a viscous component and a wave making component. The first will largely dominate in most cases, given the relatively small velocities of the current. The viscous component may be further separated in two main contributions, namely viscous drag and skin friction. The first dominates for bluff bodies and the second for streamlined bodies.

Presently, model testing is the most reliable method to estimate the current loads. These can be performed in wind tunnel facilities, or in towing tanks. However, given that current steady loads may be of relatively small importance for floating bridges, approximated methods may be appropriate. In fact, several existing floater designs consist of streamlined bodies which are aligned with the current. In this case, the current steady forces are expected to be small compared to the other steady environmental forces. Still, the relative importance of current steady forces depends of the floater geometry and current velocity and needs to be checked before an approximate approach is applied.

Approximate semi-empirical methods from the offshore industry may be used, provided the body geometry is similar enough to those of the offshore structures (which often might not be the case).

For streamlined floating bodies, use of empirical formulas to calculate current forces on FPSOs may be considered (FPSO – floating, production, storage and offloading). In this case, the longitudinal direction horizontal force is mostly related to skin friction and can be represented by:

$$F_{Xc} = \frac{1}{2}\rho S U_c^2 C_F$$

where ρ represents the water density, U_c the current velocity, S the wetted surface and C_F the frictional coefficient to be determined by the ITTC 1957 formula:

$$C_F = \frac{0.075}{(log_{10}R_n - 2)^2}$$

This formula includes a global form effect increasing the value of C_F compared to the value for flat plates as presented by (Hughes, 1954).

(Bertram, Practical Ship Hydrodynamics, 2000) describes this method, together similar alternative methods. In case the current is not aligned with the streamlined body, (Faltinsen O. M., 1990) provides an approach to calculate the transverse force and yaw moment based on the cross-flow principle and the Munk moment.

Current loads on floaters consisting of an assemble of slender elements can be estimated based on a strip-wise approximation of the elements and the related 2D cross sectional forces. One example are floaters with semi-submersible type of configuration, composed of columns and pontoons. The current velocity is decomposed into one component in the cross-flow direction of the slender element and one component in the longitudinal direction. The first component causes separation and it is estimated based on 2D drag coefficients, which need to be pre-determined. The longitudinal direction component results on shear forces only and it may usually be neglected. More details and discussion on the method can be found in (Faltinsen O. M., 1990).

Computational fluid dynamics (CFD) is certainly a possibility to calculate current loads with the potential to provide accurate results. If the geometries and/or flow conditions are not similar to cases where CFD models have been validated before, validation based on comparison with test data is recommended.

Current induced vortex shedding over bluff bodies, such as circular cylinders, may induce inline and/or cross flow oscillatory forces. If the period of the forces is close, or crosses, the floating system natural period, both inline and cross flow motions may be generated. These are named vortex induced motions (VIM)I. The cross flow motions are usually larger than inline. One important parameter is the reduced velocity:

$$V_R = \frac{U_c}{f_n D}$$

where U_c is the current velocity, f_n the natural frequency of body motion and D the body diameter.

For V_R smaller than approximately 3-4, VIM motions are small and inline with the current. For V_R larger than 3-4 cross flow motion will start in combination with in line motion. The motion magnitudes may be significant.

Since vortex shedding is a highly nonlinear phenomenon, there are no reliable numerical methods to estimate VIM. Furthermore, existing prediction methods are based on empirical data, which may be inappropriate for floaters of floating bridges. The current practice is to use model test data in combination with experience. CFD modelling may also be used in combination with model testing and empirical models. For rounded shapes, the vortex shedding depends strongly on the Reynolds number, therefore the model tests need to be planned carefully and the test data might need interpretation.

For floaters of floating bridges, in case the geometry is prone to vortex shedding, one may check the reduced velocity and the possibility of cross-flow VIM. Assuming, for the sake of example, a natural frequency of the transverse vibrations of the pontoon of 0.10 Hz, a diameter of 10 m and a current velocity of 2 m/s, then a conservative estimate of the reduced velocity is 2. It is not likely that VIM is a problem for floating bridges.

3.2.3 Wave loads – general

The floaters of large floating bridges may be considered large volume structures, since the characteristic floater dimensions are on the order of magnitude of the typical wave lengths. This means the hydrodynamic wave loads are within the diffraction wave force regime, where inertia effects dominate and viscous effects (drag) are of lesser importance.

Wave loads on large volume structures can be calculated by methods based on potential flow theory, which solve the radiation/diffraction problem. If the first order problem is solved one obtains the liner excitation and responses and the second order mean wave drift force coefficients. If the problem is solved up to the second order for pairs of harmonic incident waves, then the wave excitation includes also difference frequency components, related to low frequency forces, and sum frequency components, related to sum frequency forces.

The basic assumption of potential flow theory is that the fluid is incompressible and (basically) inviscid. Most commonly, the potential flow problem is solved by boundary element methods (BEM). The velocity potential is represented by a distribution of sources on the mean body wetted surface and it satisfies the Laplace equation in the fluid domain and conditions on the boundaries surrounding a volume of fluid. When the source function satisfies the free surface condition, it is named Green function. One alternative consists of using simple Rankine sources distributed over the mean body surface and free surface. Complying with the boundary condition on the body surface (Green function), or both on the body and free surfaces (Rankine function), results on an integral equation for the unknown source strength. The latter boundaries are discretized into panels, which results in a set of equations to be solved for the source strength.

Details on the formulation for panel methods based on the Green function approach can be consulted, for example, in (Lee C. H., 2004) and (Lee C. , 2007). The Rankine source approach have been used and described, for example, by (Bertram, Ship motions by a Rankine source method, 1990). Most of the available codes are based on the Green function approach (see also Section 4.2). Since there is no need for meshing the free surface and checking convergence of the results related to representation of free surface effects, Green function based methods are easier to use. Rankine source methods may present advantages for solving the forward speed problem, or the equivalent wave-current interaction problem, since it is easier to comply with complex free surface conditions. For this reason, such methods have been applied mostly for ships. Another advantage of the Rankine source methods is that they do not suffer from the irregular frequencies problem, contrary to the Green function methods (additional discussion on this topic ahead).

The integral equation for the unknown source strength becomes singular as the thickness of the body decreases. However, thin bodies might need to be modelled in case, for example, floating bridges include floaters with heave plates to control the added mass and damping. To avoid the referred singularity, thin elements may be represented by a distribution of dipoles. The body surface is therefore represented by a combination of both sources and dipoles (Lee C. H., 2004).

Most available codes discretise the body mean wetted surface into flat panels, or low order panels, meaning the source density is constant over each panel. It is also possible to represent the body boundary by higher order panels with a non-uniform distribution of source density (Lee C.-H. M., 1997). The same accuracy can be achieved with quite smaller number of panels, which may be interesting for solving complex systems with multi-body interactions. This might be the case for the floaters of large floating bridges, if the spacing between floaters is not large compared to the floater dimensions.

The relevance of potential flow multi-body interactions between floaters should always be checked, before a possible decision to neglect such effects is made. Even if the separation between floaters appears to be large, compared to the floater dimensions, the interference effects might be important. Reference is made to an experimental and numerical study with a restrained half sphere subjected to periodic waves (Zhao R. F., 1988). The body diameter was 1 meter, while the tank width was 10 meters. The tank lateral vertical walls simulate an (infinite) array of inline bodies separated by 10 m. The separation is one order of magnitude larger than the body diameter. The results show surprising strong interference effects, as can be observed in the graphs of Figure 4 with first order wave exciting drift forces and surge wave drift forces in periodic waves.

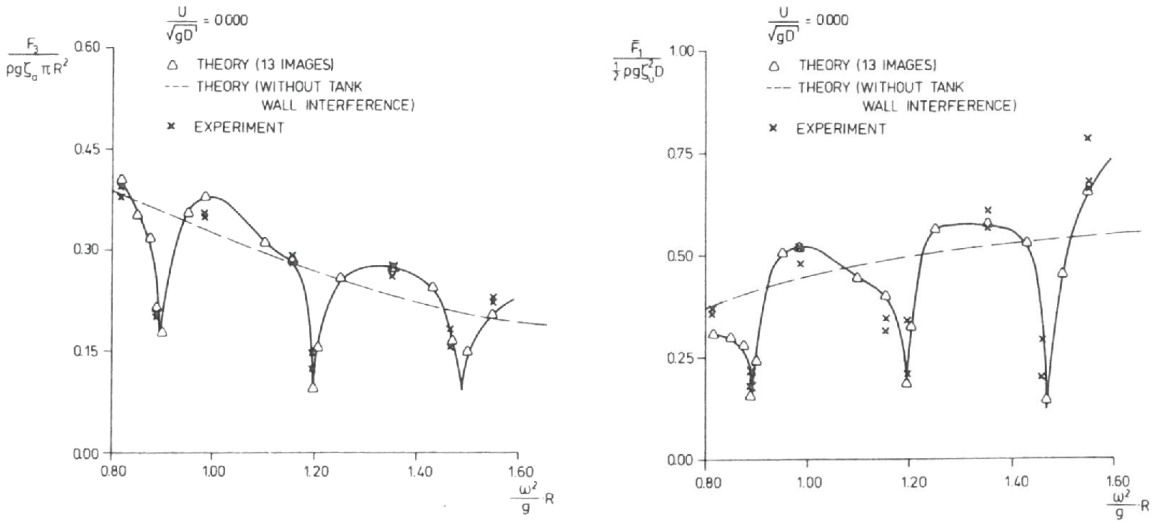

Figure 4:Comparison between experimental and numerical results for first order wave exciting heave force (left graph) and horizontal drift forces (right graph) on a hemisphere in periodic waves. Tank wall effects are accounted for (graphs from (Zhao R. F., 1988)).

Finite water depth effects influence the hydrodynamic loads on floaters and may need to be considered. The effects increase with decreasing frequency. As a reference, depth effects are assumed to influence wave kinematics when the water depth is smaller than half the wave length. The actual influence on the hydrodynamic loads depends on the floater geometry and load of interest. In addition, if the floater is located near the coast with variable bottom bathymetry, the variation may significantly influence the floater motions, as compared to a constant water depth. One possibility is to model the bottom in the radiation/diffraction analysis by meshing an additional bottom boundary (see for example (Ferreira, 2009)). Such analysis brings considerable additional modelling and computational effort and needs to be judge based on the benefits versus the difficulties of modelling and uncertainty of the numerical results.

The actual relevance for floating bridges has not been assessed and it might be that such effects are not important, since floaters are used because the water depth is large. If finite water depth effects are relevant, it

is possible to say that, for practical applications, they can be calculated with radiation/diffraction codes for horizontal sea bottoms only. Therefore, the following effects cannot be represented:

- Effects of the varying bathymetry on individual floaters.
- Effects of the varying bathymetry on multi-body interactions. Interactions between floaters are calculated either for a finite horizontal water depth, or for infinite water depth.

It might be that appropriate approximations provide accurate results, but studies on this aspect are lacking.

Existence of irregular frequencies is a well-known problem of codes applying the free surface Green function method. Bodies with large waterplane area are prone to such results. The problem is related to no solution, or non-unique solution of the boundary integral equations at a set of irregular frequencies. These correspond to eigen frequencies where the fluid and the free surface are inside the body. Results for these frequencies are wrong, from the physical point of view. Several numerical methods were proposed to suppress the irregular frequencies (Lee C.-H. a., 1989). Imposing an additional homogeneous Neuman boundary condition on the interior free surface has shown to be an efficient solution.

For typical offshore structures, irregular frequencies often occur at relatively high frequencies, compared to the wave frequency responses of interest, and in this case do not pose significant problems. However, it might be that special care dealing with irregular frequencies is required for floating bridges, given the large number of system natural frequencies, related to the bridge natural modes and, possibly, to entrapped wave modes in between floaters.

It is important to note that even large volume structures may be subjected to non-negligible viscous effects. These may contribute to the overall damping of the system, or to both the damping and the wave excitation. The state-of-the-art approach is to represent the additional viscous effects by semi-empirical models and combine them with the potential flow forces in the equations of motion. Frequency domain solution of the motion equations require linearized coefficients, while nonlinear force models can be used in time domain methods (as for example quadratic damping coefficients). In case the floater also includes slender elements, the related wave loads can be calculated by a Morison model. Viscous effects on the large volume body, i.e. skin friction, hull generated eddies, vortices from bilge keels, need to be determined empirically, or by (carefully) using CFD.

Finally, the mooring lines dynamics contribute to the "dampen" the motions of the floater. Such effects are expected to be negligible for the floating bridge wave frequency motions, while they probably have an influence on the low frequency motions. Viscous damping effects from the mooring lines need to be assessed and included in the LF solution if relevant. Hydrodynamic inertial effects from the mooring lines are expected to be small.

3.2.4 Wave frequency loads

The wave frequency loads on large volume structures are usually calculated by Green function potential flow codes assuming linearity with respect to the wave amplitude. Besides incompressibility and inviscid fluid requirement, linearity requires small amplitude waves (low steepness) and small amplitude motions. The potential flow problem boundary conditions are linear, meaning they are enforced at their mean positions (mean body wetted surface and mean water level). The waterplane area is assumed constant during the motion.

The linear hypothesis for calculation of first order potential flow quantities, such as added masses, radiation damping coefficients and wave exciting forces, is expected to be valid for floaters of floating bridges. Given the protected location of floating bridges, the wave amplitudes are expected to be relatively small. Additionally, the floater WF motions are of small amplitude since they are constrained by the connection to the bridge columns and girder.

First order linear results consist of added mass, damping coefficients and wave exciting forces. Mean wave drift forces are calculated from first order quantities, although they represent a second order result (proportional to the wave amplitude squared).

As referred above, depending on the floater geometry and details, viscous drag effects may need to be considered for the calculation of wave frequency damping and/or wave excitation. The relative importance of

viscous effects increases with the motion amplitude and with the frequency. For floating bridges, wave amplitudes and motion amplitudes are small, therefore it is not obvious that wave frequency viscous effects are important and further studies are needed.

3.2.5 Low frequency wave loads

Low frequency motions of moored structures occur as frequencies significantly lower than the wave frequencies. Slowly varying wind loads and wave loads are responsible for the LF motions. This Section focus on wave loads. Although slowly varying wave drift loads are quite small, compared to wave frequency loads, they often excite moored structures at their natural frequencies. If the LF damping is small, then the motion amplitudes may be large.

In the case of large floating bridges, low frequency wave loads may excite the first modes for deflections about the girder strong axis (bridge horizontal modes). For this reason, horizontal wave drift forces may be important. The related LF motion responses should always be checked and included in the global analysis is found to be relevant. Given the natural frequencies of the floater vertical motions and angular motions, vertical drift forces and all drift moments are not seen as relevant for floating bridges, at least for the concepts known by the authors.

Assuming small amplitude incident waves, perturbation analysis results on slowly varying wave drift forces proportional to the wave amplitude squared. For long-crested seastates, the slowly varying force in the *k*-direction is given by superimposing the effects of many pairs of incident harmonic wave components:

$$F_k(t) = \sum_{m=1}^{N_w}\sum_{n=1}^{N_w} A_m A_n \left\{ \begin{array}{c} QTF_k^{re}(\omega_m,\omega_n)cos[(\omega_m-\omega_n)t+(\phi_m-\phi_n)]+ \\ +QTF_k^{im}(\omega_m,\omega_m)sin[(\omega_m-\omega_n)t+(\phi_m-\phi_n)] \end{array} \right\}$$

where N_w is the number of harmonic wave components representing the irregular wave, A_m and A_n are the wave amplitudes of the harmonic components m and n, ϕ_m and ϕ_n the related random phase angles and QTF_k^{re}, QTF_k^{im} the real and imaginary parts of the wave exiting force quadratic transfer function (QTF). The LF force oscillates at the difference frequencies $\omega_m - \omega_n$.

For short created waves, meaning multiple directional irregular waves, the wave drift force is given by a quadruple sum:

$$F_k(t) = \sum_{m=1}^{N_d}\sum_{n=1}^{N_d}\sum_{i=1}^{N_m}\sum_{j=1}^{N_n} A_{mi}A_{nj} \left\{ \begin{array}{c} QTF_k^{re}(\omega_{mi},\omega_{nj})cos[(\omega_{mi}-\omega_{nj})t+(\phi_{mi}-\phi_{nj})]+ \\ +QTF_k^{im}(\omega_{mi},\omega_{nj})sin[(\omega_{mi}-\omega_{nj})t+(\phi_{mi}-\phi_{nj})] \end{array} \right\}$$

where N_d is the number of wave directions and N_m, N_n are the numbers of wave components in the m^{th} and n^{th} wave directions. In the most general case, the exciting force QTFs are a function of four variables: ω_m, ω_m, β_m and β_n. The complete calculation of LF wave drift forces in directional seastates is extremely time consuming. In practice, it is not used. Calculation of such forces in directional waves based on approximations for the full QTFs, such as Newman's approximation (Newman J. , 1974), are possible and some software provide this option. In practice, directional waves are not usually considered for calculations of QTFs in the context of wave drift forces simulation.

3.2.6 Wave drift force coefficients

There are two main methods to calculate wave drift force coefficients, the "far-field" method and the "near-field" method. The first is based on the time rate of change of the momentum in the fluid within a control volume limited by a vertical boundary located far away from the body (e.g. (Faltinsen O. M., 1974), (Lee C. H., 2004)). The method gives only the mean wave drift coefficients in harmonic waves for the horizontal modes (arbitrary shaped bodies). Calculations are robust and easy to converge. Some codes offer the possibility to model control surfaces around the body, which provides mean drift force coefficients for the vertical modes by the momentum method as well. Mean wave drift forces require solution of the linear boundary value problem only, since they depend of first order quantities only.

The near field method was introduced to evaluate the mean wave drift forces in all six degrees of freedom, as well as the sum and difference frequency wave load components. The results are the full QTFs and achieving these requires solving the second order boundary value problem. Available commercial software uses the Green function method. The Green function satisfies the linear free surface only, therefore, complying with the second order free surface condition requires meshing of the free surface. The method requires that all pressure contributions to second order terms are correctly integrated over the instantaneous (2nd order) wetted surface (e.g. (Pinkster J. V., 1977), (Lee C. H., 2004)). Numerical schemes are sensitive to the meshing and convergence is significantly more difficult than for far-field methods. More recently, the "middle-field" formulation was proposed to overcome the convergence problems (Rezend, 2007).

When drift forces are calculated by the near-field method, or by the middle-field method, it is good practice to check the results by comparing mean wave drift force coefficients with those from the far-field solution (in addition to convergence checks).

Restricted water depth effects on the hydrodynamic loads are referred on Section 3.2.3. It worth mentioning that water depth effects indeed have an important influence on the wave drift forces.

The wave drift force coefficients depend of the first order motions, which means that, if relevant, viscous effects must be realistically included in the first order frequency domain analysis before drift force coefficients are computed.

3.2.7 Approximations for calculation of wave drift forces

Solving the full second order potential flow problem is computationally demanding. Achieving converged results is often not easy. Only a few commercial codes offer the option to solve the full second order problem. In practice, there are many cases where the full solution is not needed, and approximations provide good results. Two well-known approximations have been proposed by Newman (Newman J. , 1974) and Pinkster (Pinkster J. , 1980). An interesting more complete approximation is described in (Lee C. , 2007). More details and additional possibilities can be consulted in (de Hauteclocque, 2012) and (Pessoa, 2013).

The following paragraphs describe the most used approximations.

Newman's approximation

The simplest method to calculate the slowly varying wave drift forces uses the mean wave drift force coefficients only (Newman J. , 1974). The QTF off diagonal terms, corresponding to finite difference frequencies, are approximated by the main diagonal terms, or zero difference frequency terms. While different variants of the approximation have been proposed, the following is probably the most common:

$$QTF_k(\omega_1, \omega_2) = 0.5[QTF_k(\omega_1, \omega_1) + QTF_k(\omega_2, \omega_2)]$$

where ω_1 *and* ω_2 are the frequencies of the pair of incident harmonic waves.

Calculation of the zero difference terms, or mean wave drift force coefficients, is relatively simple since there is no need of solving the second order problem. The coefficients are given by quadratic terms calculated from first order quantities related to mono-chromatic waves, therefore only the linear problem requires solution. Furthermore, the more robust momentum methods can be applied.

Although application of Newman's approximation brings significant advantage, it is recommended that the applicability is checked case by case. It is usually assumed that the approach is accurate enough if:

- The system is moored in deep water. Restricted water depth increases significantly the second order incident wave potential and related LF excitation.
- The relevant LF response occurs at very low frequencies (difference frequencies "close" to the main diagonal). This implies that the system natural period is long.

Recent studies show that complying with these assumptions might not be enough to achieve accurate results, namely when the full QTF presents large off-diagonal variations around the main diagonal ((Fonseca, Wave drift forces and low frequency damping on the Exwave FPSO, 2017)). Furthermore, the accuracy is very much dependent on the seastate peak period. It is therefore recommended that applicability of Newman's

approximation is checked against results from a more complete solution. Such check can be done, for example, by comparing the drift force spectra around the natural frequency, from the approximation and from the full 2nd order solution. Figure 5: Surge load spectra for a FPSO moored in deep water – comparison between predictions based on full QTFs and on Newman's approximation. Left and right graphs corresponding to wave peak periods of respectively 12 and 16 seconds.

illustrates with one example for a FPSO. The graphs show the surge wave exciting force drift spectra for an FPSO in head waves. The left graph corresponds to a wave peak period of 12 s and the right graph to 16 s. Three lines stand for results using the full 2nd order QTF ("Full QTF – Chen"), Pinkster's approximation and Newman's approximation. The surge natural frequency of 0.5 rad/s is highlighted in the graphs. Newman's approximation is slightly conservative for the 12 s seastate and it is un-conservative for the 16 s seastate.

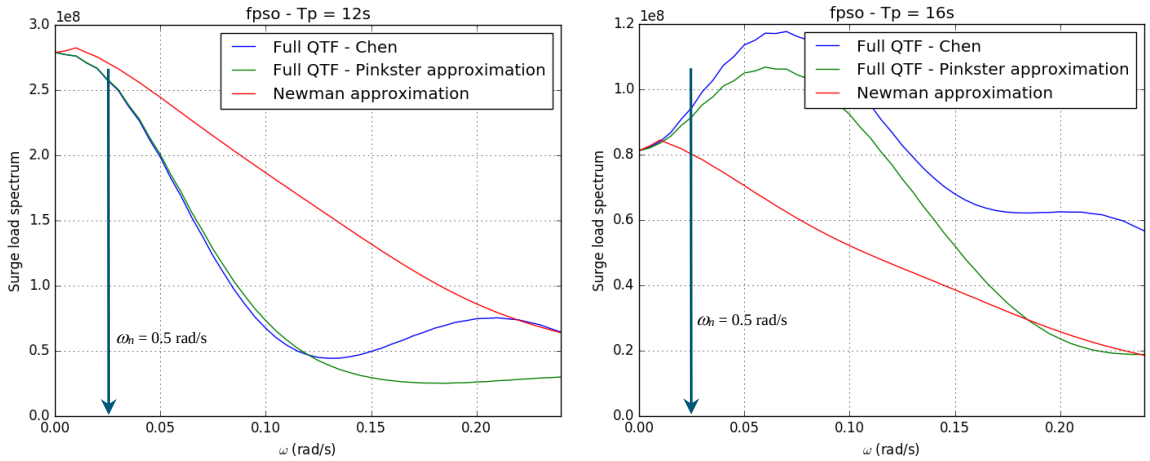

Figure 5: Surge load spectra for a FPSO moored in deep water – comparison between predictions based on full QTFs and on Newman's approximation. Left and right graphs corresponding to wave peak periods of respectively 12 and 16 seconds.

Newman proposed one more simplification, in this case to speed up the simulation of wave drift forces in the time domain. Simulation of the wave drift forces applying the double-sum presented in Section 3.2.5 is time consuming, especially for long time histories. Given the typical long natural periods excited by the low frequency forces, 3 hours full scale is usually considered the minimum duration to achieve reasonable statistics. Computational effort is significantly reduced by replacing the double-sum formula by a square of a single sum (Newman J. , 1974):

$$F_k(t) = 2\left\{\sum_{j=1}^{n} A_j\left[QTF_{jj}^{re}\right]^{0.5} cos\left(\omega_j t + \phi_j\right)\right\}^2$$

The above formula includes un-physical high frequency effects, which are filtered out when computing the low frequency motions.

There is another alternative to the double summation computation, which does not introduce an approximation like the previous formula. It consists of a single summation together with Fourier transform, using the QTF property that the diagonals coefficients have constant frequency. See, for example, (Agarwal, 2011), for details.

Pinkster's approximation

The second order force (or moment) can be decomposed into two parts: the first is related to quadratic interactions of first order quantities, F_q, and the second is due to second order potentials, F_p, (Lee C.-H. , 1995):

$$F\left(\omega_i, \omega_j\right) = F_q\left(\omega_i, \omega_j\right) + F_p\left(\omega_i, \omega_j\right)$$

Pinkster's approximation provides a simplified way of calculating the force contribution related to second order potentials (Pinkster J. , 1980). The assumption is that the second order incident wave potential gives the largest contribution to F_p. The second order potential force is approximated as (de Hauteclocque, 2012):

$$F_p(\omega_i, \omega_j) = C(\omega_i, \omega_j) F^{(1)}(\omega^-)$$

where $F^{(1)}$ is the first order wave exciting force ratio amplitude operator (RAO) and $C(\omega_i, \omega_j)$ is the ratio between the second order incident wave potential and the first order incident potential:

$$C(\omega_i, \omega_j) = \frac{ig\omega^-}{g(k_i - k_j)tanh(k_i - k_j)h - (\omega_i - \omega_j)^2}$$

where k_i is the linear wave number corresponding to an angular wave frequency ω_i, h is the water depth and ω^- is the solution of:

$$(\omega^-)^2 = g(k_i - k_j)tanh(k_i - k_j)h$$

In principle, codes based on Pinkster's approximation calculate the QTF terms representing the quadratic interactions of first order quantities, $F_q(\omega_i, \omega_j)$, in a complete manner (and not applying Newman's approximation), while $F_p(\omega_i, \omega_j)$ is given by the formulas above. The result is the full QTF, with approximation of the second order potential flow terms.

Pinkster's approximation provides a significant improvement for cases where Newman's approach is insufficiently accurate. The QTF predictions tend to deviate from the complete second order solution as the difference frequency increases. In practice, the approximation works fine for many applications where the system natural period is long. Figure 5 compares surge drift force spectra calculated from Newman's approximation, Pinkster's and complete second order solution. One observes good predictions by Pinksters' approach for frequencies below around 0.15 rad/s (T = 42 s).

3.2.8 Wave drift damping

Methods to calculate wave drift force coefficients account for the wave frequency motions only and the body is assumed to be oscillating with wave frequency motions around its mean position. The low frequency wave excitation induces low frequency motions which may be significantly larger than the WF responses. As the body moves through the first order scattered wave field with WF motions, it experiences some LF potential flow damping.

Another way of looking at the problem consists of observing that the LF velocities modify the wave drift forces, as compared to the idealized condition used for computation of wave drift force coefficients. The modification of drift forces is partly due to Doppler effects, as the frequency of encounter between the body and the waves depends of the LF velocity. There is also a dynamic effect. Assuming a quasi-steady approach, the wave drift damping is derived from the rate of change of the wave drift forces in waves (or added resistance) with respect to a small body velocity:

$$B_{kj}(\omega, \beta) = -\frac{\partial F_k(\omega, \beta)}{\partial U_j}\bigg|_{U_j=0}, \qquad k, j = 1, 2, 6$$

The problem can be solved with a wave-current potential flow panel method – see following Section. In case wave-current codes are not available, approximate wave drift damping coefficients may be estimated with formulae based on Aranha's formula (see Section 3.2.9).

Although there are no specific studies on wave drift damping effects on the estimation of low frequency responses of floating bridges, it is expected that such effects are important and should not be neglected. The other sources of damping are small, so the relative importance of the wave drift damping might be significant: the radiation damping is negligible for long periods, the pontoon viscous damping is probably very small for streamlined hulls and the mooring line damping is not expected to be large due to small number of lines, intermediate water depth and small motion amplitudes (the line damping is quadratic).

3.2.9 Wave-current interactions

General

The current has a significant impact on the low frequency wave drift forces and a smaller effect on the first order responses. In general, the wave drift forces increase for waves and current in the same direction and they decrease for waves and current in the opposite direction. The effects increase with the current velocity. Figure 6 illustrates the wave current interaction effects on a hemisphere restrained to move on the left side graph and free to move in surge and heave on the right side (Zhao R. F., 1988). The values are based on potential flow calculations. The plots show the mean wave drift force coefficients as function of the nondimensional wave frequency for different current velocities (R and D stand for radius and diameter). Positive current means it propagates in the same direction as the waves.

The graphs show the current clearly modifies the wave drift forces. Assuming as reference a current velocity of 1 m/s and a floater width of 10 meters, which may be considered representative of floating bridges floaters, then $U/\sqrt{gD} = 0.10$, therefore a value even larger than those presented in the graphs. In case a current is present, its effects on the wave drift forces need to be assessed and, in principle, included in the numerical model.

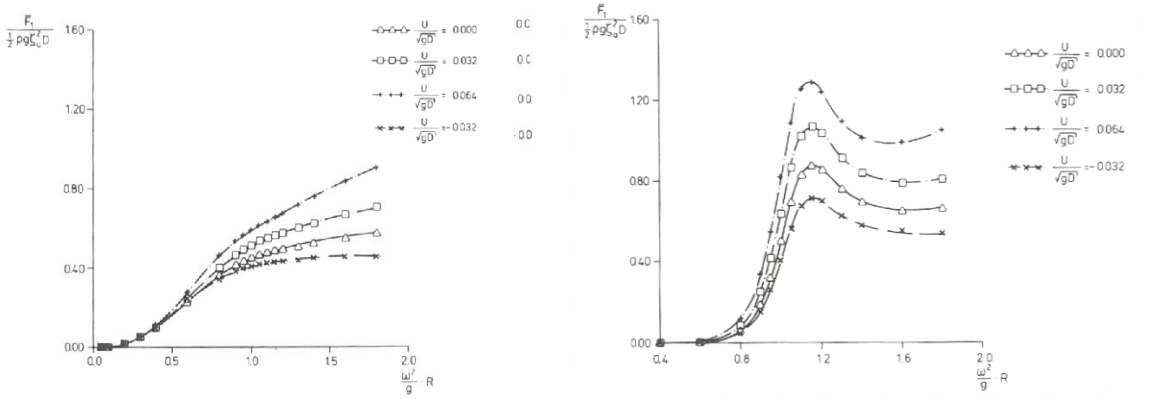

Figure 6: Horizontal mean wave drift force on a hemisphere in collinear waves and current. Left graph correspond to the restrained body and right graph for the body free in surge and heave (graphs from (Zhao R. F., 1988)).

Potential flow numerical methods

Several authors formulated and solved the first order wave-current potential flow problem, as for example (Zhao R. a., 1989), (Grue, 1993), (Chen X. B., 1998), (Hermundstad, 2016). These methods generalize the radiation/diffraction solutions for conditions without current. One assumption is that the current velocity is small, or more precisely, the Brard number is small:

$$\tau = \omega_e U_c / g$$

where ω_e is the frequency of encounter. Given the wave systems represented by the common formulations, the solution is limited to $\tau < 0.25$. In practice, depending on the formulation and related simplifications introduced to represent the interactions between the steady and unsteady flows, the limiting Brard number might need to be lower than 0.25. For this reason, existing codes provide good results for low frequencies and the accuracy reduces as the frequency increases above a certain value, which depends on U_c.

While zero current potential flow panel methods require meshing of the mean wetted hull only, wave-current interaction codes need meshing of the free surface also. This is related to the more complex free surface boundary condition which accounts for interactions between the steady (*Uc*) and unsteady flows. The applied Green function is still the stationary Green function. The computational effort increases compared to the zero-current solution.

Aranha's formula

One simplified alternative to the use of wave-current interaction codes consists of using Aranha's approximation (Aranha J. , 1996), (Aranha J. a., 1997). The formula gives the horizontal wave drift forces on a body in harmonic waves in the presence of current, $F^{(c)}$, given the same forces without current, $F^{(0)}$:

$$F^{(c)}(\omega, \beta, U_c, \alpha) = [1 + 4\tau cos(\beta - \alpha)]F^{(0)}(\omega_e, \beta_r)$$

where ω is the wave frequency, β the wave direction, U_c the current velocity, α the current direction, τ is the Brard number. ω_e is the frequency of encounter and β_r the refracted wave direction:

$$\omega_e = \omega + \frac{\omega^2}{g} U_c cos(\beta - \alpha)$$

$$\beta_r = \beta - \frac{2\omega U_c}{g} sin(\beta - \alpha)$$

The formula above modifies the no current drift forces in two ways: (a) the frequency and heading are corrected to account for doppler effects, (b) a dynamic correction is added.

Aranha's formula assumes of small Brard's number. For a given current velocity, the accuracy reduces as the frequency increases. In practice, a limiting Brard's number of 0.1 may be taken as reference. The limitation may be challenging for floating bridges, where the design current velocities may be relatively high, while the seastate frequency content is also high. As an example, considering U_c = 1 m/s, the limiting Brard's number of 0.1 gives a minimum harmonic wave period of 7 s.

Furthermore, the formula was derived for deep water waves. It may be considered valid for $h/\lambda > 0.5$ (h and λ stand for water depth and wavelength).

For the surge and sway forces, the expression above can be written as:

$$F^{(c)}(\omega, \beta, U_c, \alpha) = F^{(0)}(\omega_e, \beta_r) + \begin{bmatrix} B_{11} & B_{12} \\ B_{21} & B_{22} \end{bmatrix} \begin{bmatrix} U_c sin\alpha \\ U_c cos\alpha \end{bmatrix}$$

where B_{kj} are the wave drift damping coefficients. Details on the formulae to calculate the wave drift damping coefficients based on Aranha's formula can be consulted in (Kim, 1998), including also the yaw drift moment and generalization for finite water depth.

3.2.10 Viscous effects on wave drift forces

Viscous effects may contribute to the wave drift forces. In some conditions, viscous drag may in fact dominate. Viscous drift is associated with flow separation and drag forces which do not balance to zero over the wave cycles. For conditions without current, they may be considered relevant if the wave amplitude is large compared to the cross-section dimension of the floater components. Occurrence of flow separation is a function of the Keulegan-Carpenter number, which expresses the relative importance of drag forces over inertia forces:

$$KC = U_m T/D$$

where U_m is the maximum wave orbital particle velocity, T is the wave period and D the representative cross section dimension.

The flow separates from the body for sufficiently large KC numbers. As a reference, for a circular cylinder, the flow separates for KC values larger than 2-3. Once there is separation within the oscillatory flow, viscous drift may result from different mechanisms. Viscous effects at the free surface zone have been identified to be important for vertical cylinders (Dev, 1994). In this case, viscous drift forces are of third order, therefore proportional to the cube of regular wave amplitude. Cross flow effects on submerged slender elements may also contribute. These aspects are discussed in (Faltinsen O. M., 1990).

Initiation of flow separation is more complex in the presence of current. It depends of, at least, the KC number and the ratio U_c/U_m, where U_c is the current velocity and U_m is the maximum wave orbital particle velocity.

For large U_c/U_m it is expected that flow separation occurs for all *KC* values. In reality, it is likely that flow separation occurs when the relative flow velocity does not change sign during the wave cycles, meaning approximately $U_c/U_m > 1$.

In the presence of current, if there is flow separation and the wave particle velocities are of the same order of magnitude of the current velocity, there will be viscous drift forces even for fully submerged bodies. This is due to non-zero mean value of oscillatory component of the total velocity squared. For sake of simplicity and to neglect local flow effects, let's assume a slender element. In harmonic waves the drag force is proportional to:

$$U|U| = \big(U_c + U_m sin(\omega t)\big)|U_c + U_m sin(\omega t)|$$

The mean value of the former expression may be significantly larger than U_c^2 due to combination of the current with the waves. The difference is related to viscous drift.

In practice, for floaters of floating bridges, the wave amplitudes and wave lengths are small compared to typical floater dimensions. For this reason, viscous drift is not expected to be significant for conditions without current. The conclusion might be different for configurations including, for example, surface piercing columns.

For conditions with current, relevance of viscous drift depends on the floater geometry and typical wave periods. Viscous drift may be present for floaters prone to separation with the current, if the wave periods are sufficiently long. For some of the known floater designs, which consist of large volume structures (compared to predominant wave lengths) it is expected that drift forces are dominated by potential flow effects. Furthermore, known concepts consist of floaters streamlined in the current direction, therefore viscous effects are expected to be small.

3.2.11 Sum-frequency wave forces

Second order sum-frequency wave exciting forces result from interactions of pairs of harmonic wave components composing the irregular seastates. The related frequencies are typically above the wave frequency range, or on the tail of the wave spectrum. Sum frequency forces are relevant in case they may excite high frequency motion responses, meaning in case some of the floater natural frequencies are high. This is the case for the vertical motion responses of tension leg platforms (TLPs).

For floating bridges, second order sum-frequency wave forces on the floaters are expected to be small, since the waves are of small amplitude. However, given the multitude of bridge eigen modes including many with high frequencies, it might be of interest to check is springing responses are excited. Note that floater motions of small amplitude and high frequency are very lightly damped.

3.2.12 Inhomogeneous wave and current loads

Inhomogeneous wave and current loads, due to inhomogeneity of environment along the bridge span, need, in principle, to be considered. Compared to homogeneous conditions, inhomogeneity changes, at least:

- The magnitude of loads along the bridge.
- The loads frequency content in time and space.

Such differences might have an important effect on the magnitude of the bridge motion responses (and internal loads) and on the natural modes that are excited.

The problem of inhomogeneous wave and current loads is very much related to the consistent description of the environment along the bridge and to the capability of the global analysis software to account for different environments along the bridge span. In between these two steps, we have the calculation of current and wave loads coefficients.

Calculation of current load coefficients for inhomogeneous currents is not seen as a problem, assuming the current is nearly perpendicular to the bridge girder and interference between pontoons (blockage) is either negligible, or it is similar to the homogeneous case. Such simplifications are possible because the current steady loads are expected to be small, compared to the other steady environmental loads.

On the other hand, calculation of wave load coefficients for inhomogeneous wave fields is not straight forward with today's numerical tools (for a known inhomogeneous wave field). The problem lies in the calculation of wave exciting forces by frequency domain (FD) radiation/diffraction codes (we will not discuss time domain solutions, since they seldom are used in practice). These codes solve the diffraction boundary value problem for "homogeneous" harmonic incident waves of unit amplitude. This limitation has the following consequences:

(a) If the global analysis is performed in the frequency domain, then, in principle, the global analysis is connected to the diffraction solution, and the solution is obtained frequency by frequency for harmonic waves (the wave field is homogeneous).

(b) If the global analysis is performed in the time domain, then, depending on the actual software, it might be possible to consider different seastates for different pontoons in the global analysis. This solution is consistent if interaction effects between pontoons can be neglected.

(c) If the global analysis is performed in the time domain and interactions effects between pontoons are relevant, then solution (b) is inconsistent. The diffraction interaction effects between floaters inherently assumed "uniform" harmonic waves along the whole array of floaters. If interaction effects are relevant, they will be calculated for uniform waves.
Solution (b) being inconsistent does not necessarily mean the results are un-acceptable in practice. But the approach needs validation.

4. Implemented theory in available software

4.1 Wind loads

The wind load models implemented in several commonly used software programs are summarized briefly in Table 2. There are challenges in obtaining complete information regarding all the different software tools, and such information is to the best knowledge of the authors at the time of writing.

Table 2: Wind load models in common software tools.

Program	Description/comments	Wind load models	Application examples
Orcaflex by Orcina	Time-domain wind-wave-structure (beam) analysis	NQSA	SBJ-30-C3-NOR-90-RE-100 (end-anchored)
3DFloat by IFE	Time-domain wind-wave-structure (beam) analysis	NQSA	SBJ-30-C3-NOR-90-RE-100 (end-anchored)
RM Bridge by Bentley	Hybrid FEM formulation,	CFD, FDAC	Sognefjord Feasibility Study (11258-03)
Nova-Frame by Aas-Jakobsen	Static and dynamic wind-structure analysis, frequency-domain	FDAC	SBJ-30-C3-NOR-90-RE-100 (end-anchored)
SIMA	Time-domain wind-wave-structure (beam) analysis	NQSA	(Cheng, Gao, & Moan, 2018)
Abaqus	General FEM software (time or frequency-domain)	NQSA or FDAC	(Xu, Øiseth, & Moan, 2018)

4.2 Wave and current loads

Table 3 presents the exiting computer codes for solving the wave-structure interaction problem by boundary element methods (panel methods). The list is not exhaustive, but it includes the most used software. Most software solves the boundary value problem in the frequency domain (FD) and this is considered the practical solution for engineering applications. One of the codes solves the problem in the time domain (TD).

All codes calculate the mean wave drift force coefficients.

The fourth column – Wave-current code – refers to potential flow formulations accounting for the wave-current interaction in the first order responses and mean wave drift forces. Some of the codes with the flag "No" may still account for wave-current effects through approximate methods, such as based on Aranha's approximation (see Section 3.2.9).

Regarding the last column – QTFs – it refers to whether the code calculates full QTFs of wave exciting forces, or only mean wave drift coefficients. Pinkster's approximation applies to only difference frequency forces, while the full 2nd order solution provides both difference frequency and sum frequency forces.

It is important to note that although a few codes solve the wave-current problem and calculate full QTFs, these two solutions are not provided together. Presently, there are no codes available to calculate full QTFs accounting for wave-current interactions (for practical engineering problems).

Table 3: Computer codes for solving the radiation/diffraction potential flow problem.

Computer program	Developer	Frequency / time domain	Wave-current code	QTFs
Aqwa	Ansys	FD	No	Pinkster
Delfrac	TU Delft	FD	No	Pinkster
Diffrac	Marin	FD	No	Pinkster
Diffract	Oxford University	FD	No	Full 2nd order
Diodore	Principia	FD	No	Full 2nd order
Hydrostar	BV	FD	Yes	Full 2nd order
Muldif	SINTEF Ocean	FD	Yes	No
Wamit	MIT/Wamit Inc.	FD	No	Full 2nd order
Wadam	DNV GL	FD	Yes	Full 2nd order
Wasim	DNV GL	TD	Yes	No

5. Review of methods applied for the Bjørnafjorden project

Statens vegvesen promoted the third phase concept development for a bridge crossing over the Bjørnafjord. Significant work has been produced and documented related to the bridge design requirements, methods and results. The present Section reviews this work in the aspects related to calculation of environmental loads. The reports being reviewed include:

- Statens vegvesen Design Basis (Statens Vegvesen, 2017).
- Multiconsult side-anchored floating bridge feasibility study (Multiconsult, Bjørnafjørden, straight floating bridge phase 3. Analysis and design (Base Case). Appendix B - Environmental loads analysis, 2017b).
- AAS-Jakobsen side-anchored floating bridge feasibility study (AAS-Jakobsen, Straight bridge, Navigation channel in south, 2016).
- Norconsult end-anchored floating bridge feasibility study (Norconsult, 2017).
- AAS-Jakobsen end-anchored floating bridge feasibility study (AAS-Jakobsen, Curved bridge - Navigation channel in south, 2016).

5.1 State vegvesen Design Basis

Statens vegvesen (2017) Design Basis presents a set of rules to be applied for the feasibility studies for the crossing of Bjørnafjorden with end anchored or side anchored floating bridges. This Section summarizes the points relevant for calculation of environmental loads.

Environmental loads, namely wave, current and wind loads, are included in the category of "Variable loads".

5.1.1 Determination of load actions

Regarding determination of load actions, Section 8.2, the Design Basis states that:

- The methods shall take into consideration the variation of loads in time and space. Apparently, the referred variation in space does not include non-homogeneity of environmental wave loads, as it is clear from the Design Basis MetOcean Section 1.
- Simplified methods can be applied, if it is sufficiently documented that they provide safe results.
- Nonlinear time domain methods shall be used if linearized models are not suitable. Nonlinear effects due to coupling between wind and wave loads is given as an example.
- Nonlinear results shall be verified by linearized models.
- The loads from wind, waves and current should be calculated simultaneously, if the methods provide sufficient safety in the description of the load components and the response they generate.
- If simultaneous procedures for calculation of wind, wave and current loads are not available, the response shall be calculated individually and combined with combination factors. The combination factors should be verified from a time domain analysis.
- The calculation procedure shall include possible non-linearity in the load.

5.1.2 Wind loads

The span and long natural periods of the proposed Bjørnafjorden bridge place this structure within *wind class 3* in Statens vegvesen's handbook (Statens Vegvesen, 2015). Dynamic effects must be considered, and the computations should include aerodynamic damping and stiffness reductions. Furthermore, the wind input for class 3 bridges should be based on measured wind speeds.

The available Design Basis (Statens Vegvesen, 2017) does not specify further details for the wind load calculation compared to the handbook.

Statens vegvesen (Statens Vegvesen, 2015) describes the wind loads in terms of a mean components (horizontal load, vertical load, and torsional moment) due to the mean wind speed, and fluctuating components.

$$\boldsymbol{q_{tot}} = \bar{\boldsymbol{q}} + \boldsymbol{q}(t)$$

The mean loads are given by the wind pressure (obtained from the density $\rho = 1.25\text{kg/m}^3$ and the wind speed in the main propagation direction v_m) multiplied by a load factor and a geometric length:

$$\bar{\boldsymbol{q}} = \frac{1}{2}\rho v_m^2 \begin{bmatrix} c_D h \\ c_L b \\ c_M b^2 \end{bmatrix}.$$

Statens Vegvesen's handbook doesn't explicitly describe the load calculation model for class 3 bridges, but provides a simplified model for class 2:

$$q = \frac{1}{2}\rho v_m \begin{bmatrix} 2c_D h & (c_D' h - c_L b) \\ 2c_L b & (c_D h + c_L' b) \\ 2c_M b^2 & c_M' b^2 \end{bmatrix} \boldsymbol{v},$$

where the drag, lift, and moment coefficients relate to the mean torsional rotation angle. The derivatives (c_D', c_D', c_D') are evaluated with respect to the angle of attack and computed at the mean rotation angle. The velocity $\boldsymbol{v}$ consists of the horizontal and vertical velocity components for a girder-type element.

For class 3 bridges, the load factors and aerodynamic derivatives are to be determined using section models in a wind tunnel, and a full coupling among components is to be included (see Section 3.1).

For lower classes of bridges, tabulated drag, lift, and moment factors may be applied. For thin sections, the drag coefficient approaches 1.0 and the lift coefficient approaches 0.9 (depending on the superelevation and wind angle) (Standard Norge, 2009).

5.1.3 Wave and current loads

The Design Basis (Statens Vegvesen, 2017) does not specify details, or requirements, in terms of methods for calculation of wave and current loads. Some general requirements regarding calculation of load actions are listed in Section 5.1.1.

The Design basis MetOcean, which is annexed to the Design Basis, provides wave and current information to be used for the bridge analysis and design. This information has impact on the wave and current calculation methods, namely:

- The wind sea is represented with a directional spreading function. This indicates that wave loads should preferably be calculated for short crested waves.
- Furthermore, scatter tables are provided for wind seas and for swell. Calculation of wave loads needs to be performed for combined wind and swell seas propagating in different directions.
- Waves from passing ships may have non-negligible amplitudes and periods which may amplify the moments about the bridge girder weak axis. Therefore, methods are, in principle, needed to calculate the wave loads from transient wave groups generated from ships superimposed to the wind and swell seastates.
- The current in Table 12 of the report is assumed to go in or out of the fjord, therefore nearly perpendicular to the bridge. Current in the bridge longitudinal direction is also to be considered, representing eddies and it is given as a percentage of the former.
- The design cases include conditions with non-uniform current velocity and direction along the bridge. Therefore, non-homogeneity on the current actions needs to be considered.
- There is no reliable data on the non-homogeneity of wave conditions along the bridge, therefore the wave conditions shall be assumed constant along the bridge.

5.2 AAS-Jakobsen feasibility studies

AAS-Jakobsen lead a consortium which presented feasibility studies for a straight bridge solution (AAS-Jakobsen, Straight bridge, Navigation channel in south, 2016) and a curved bridge solution (AAS-Jakobsen, Curved bridge - Navigation channel in south, 2016). The methods for determination of design loads are similar for the two sets of studies, as well as the methods for calculation of wave, wind and current loads and responses. The following pages present a summary of the methods and of some observations which are relevant for understanding the most relevant wave, wind and current load actions.

Although this review focus on wave, wind and current loads, due to the coupled nature of the loads and responses, the descriptions below start by summarizing the options in terms of global analysis.

5.2.1 Global Analysis

The global response for ultimate limit state (ULS) analysis is performed separately for the wave/current loads, the wind loads and the static loads.

For definition of characteristics loads, wave/current and wind loads are combined with combination factors. The combination factors are quantified by simultaneous wind and wave analysis in the time domain, as required by the Design Basis (Statens Vegvesen, 2017).

The ULS load combination between the environmental loads and the remaining variable loads and permanent loads is established by the Eurocode "load factors" and described in the Design Basis chapter 8.

Figure 7, reproduced from (AAS-Jakobsen, Straight bridge, Navigation channel in south, 2016), presents the method for ULS analysis and the interaction between the different analysis codes used:

- OrcaFlex calculates wave and current responses in the time domain.
- NovaFrame calculates the wind responses in the frequency domain.
- RM Bridge is applied for the static analysis.

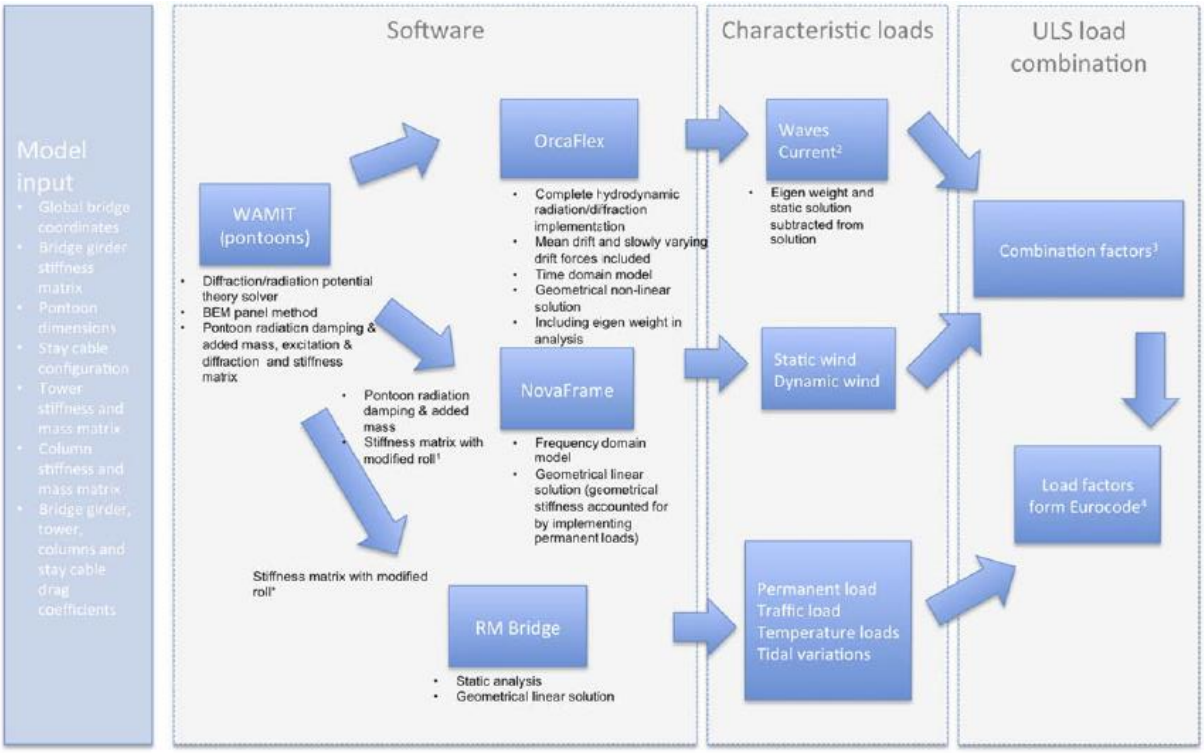

Figure 7: Method for ULS analysis and interaction between different analysis codes (AAS-Jakobsen, Straight bridge, Navigation channel in south, 2016).

5.2.2 Wave and current loads

Wave analyses are performed in the time domain with OrcaFlex considering geometric non-linear effects and mooring system nonlinear effects.

The wave loads on the pontoons are calculated by Wamit in the frequency domain and the related hydrodynamic coefficients imported into OrcaFlex to simulate the related loads in the time domain. The wave frequency loads are linear. Mean and slowly varying wave drift forces are also simulated, probably based on Newman's approximation, although not specified in the report.

Although not mentioned in the report, mean wave drift loads are probably calculated for the fixed pontoons, therefore wave frequency motion effects are neglected. The reason is that the mean wave drift loads are calculated before solving the coupled motion responses by OrcaFlex,

It is not clear if the wave energy directional spreading is taken into consideration, or not.

Wave-current interaction effects on the hydrodynamic loads is not taken into consideration. Apparently, hydrodynamic interaction effects between pontoons is neglected. It is plausible that, given the separation between pontoons of 203 m, the hydrodynamic interaction effects are not large. However, this aspect is not documented.

Regarding current induced loads, although not described in the report, these are probably based on quadratic current coefficients. The source of the current coefficients is not referred.

5.2.3 Wind loads

Wind loads were computed both using the frequency-domain wind load model in NovaFrame and in the combined wind-wave time-domain model in OrcaFlex. Although wind loads on all exposed components were considered, the results suggest that the wind loads on the girder are most important to consider.

In order to use the time domain wind load in OrcaFlex, a separate program was compiled in order to provide a wind field which accounts for spatial coherence (and is thus consistent with the NovaFrame analyses). The exact load model in the OrcaFlex analyses is not described in detail but appears to be based on NQSA.

5.2.4 Relevant observations

The analysis reports present some observations which help identifying the most relevant environmental load actions. Such information is useful for assessing the existing numerical tools and for planning the model tests within WP5. The observations include:

- Straight and curved bridges: Large moments about the bridge girder weak axis may be induced by heave and pendulum motions of the pontoons, if the natural frequencies are triggered. These are motion responses induced by first order wave loads. Heave affects the total bridge, while pendulum motion affects only the high part of the floating bridge.
- Straight and curved bridges: With a large flange attached to the bottom of the pontoons it is possible to move the natural frequencies away from the wave frequency range. The flange introduces challenges for calculation of wave exciting force and damping, due to viscous effects.
- Straight and curved bridges: The report states that "…given a design where pontoon/bridge interaction is so critical, the accuracy of hydrodynamic pontoon properties should be assessed in a tank test, especially 2nd order wave drift and viscous effects. The pontoon flange is especially critical to assess."
- Straight and curved bridges: Regarding wind responses the most important effect are the moments about bridge girder strong axis, which are dominated by the first eigen modes ranging from 32 s to 78 s. These modes are slowly varying with almost no damping (note that this conclusion is different from the one in Section 5.3).
- Curved bridge: The wave and wind induced moments about bridge strong axis are of similar magnitude and are governing for abutment and tower design.

- Curved bridge: Torque and axial load are of less importance for the ULS combination, however warping effects from the vierendel beam give some additional response locally at supports of floating bridge.
- Straight bridge: Second order wave drift loads effects on the moments about bridge girder strong axis were not assessed.
- Curved bridge: Second order slowly varying loads and responses contribute to the moment about the bridge strong axis with up to around 20 %. Wind generated waves dominate the wave drift forces.

5.3 Multiconsult feasibility study

Multiconsult lead a consortium who presented feasibility studies for a straight bridge solution (Multiconsult, Bjørnafjørden, straight floating bridge phase 3. Analysis and design (Base Case)., 2017a).

As explained before in the text, although this review focus on wave, wind and current loads, due to the coupled nature of the loads and responses, the descriptions below start by summarizing the options in terms of global analysis.

5.3.1 Global Analysis

The global dynamic analysis is performed by OrcaFlex for wave/current and wind loads and responses simultaneously and the Static analysis by Sofistik. The OrcaFlex bridge girder is modelled by beams and the columns connect the girder with the pontoon nodes where the wave and current loads are applied. Line elements represent the mooring lines and stay-cables.

Screening of worst conditions, sensitivity studies and fatigue analysis are carried out in the frequency domain, while the design load cases are analysed in the time domain.

Figure 8 presents an overview of the method for global response analysis and the interaction between the codes:

- OrcaFlex calculates wave/current and wind loads and responses simultaneously. The nonlinear coupled solution is simulated in the time domain for the design load cases, while the frequency domain linear solution is applied for screening, sensitivity studies and fatigue analysis.
- Sofistik FEM model calculates the linear permanent loads.

ULS design load checks are performed by combining load groups and load components with Eurocode load factors.

Verification of the combination factors is carried out by simultaneous calculation of characteristic environmental loads by OrcaFlex, as required by the Design Basis (Statens Vegvesen, 2017).

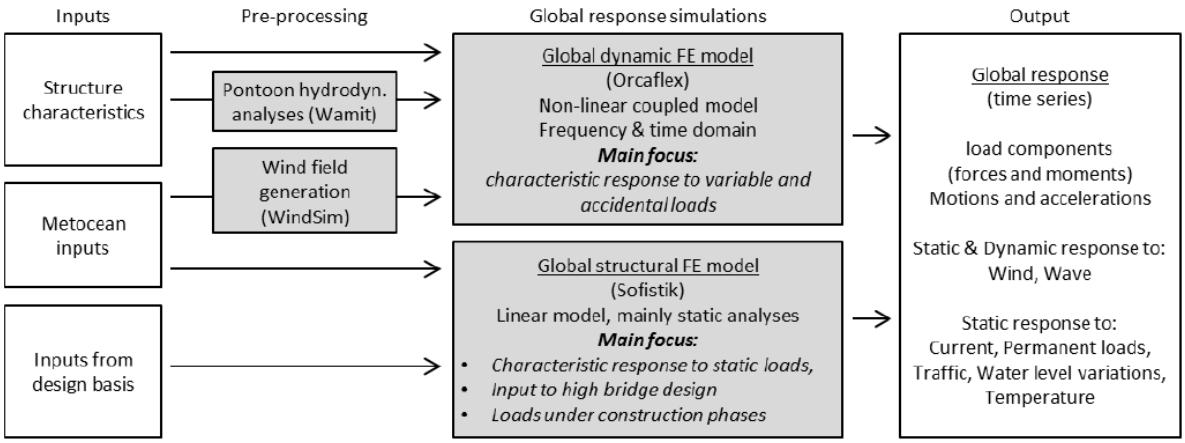

Figure 8: Method for global response analysis (Multiconsult, Bjørnafjørden, straight floating bridge phase 3. Analysis and design (Base Case). Appendix B - Environmental loads analysis, 2017b)

5.3.2 Wave and current loads

Wave analyses for the design load cases are performed in the time domain with OrcaFlex taking into account geometric non-linear effects and mooring system nonlinear restoring and hydrodynamic effects. Morison equation is used to calculate hydrodynamic loads on the mooring lines.

The wave loads on the pontoons are calculated by Wamit in the frequency domain and the related hydrodynamic coefficients imported into OrcaFlex to simulate the related loads in the time domain. The wave frequency loads are linear. Slowly varying wave drift forces are also simulated based on Newman's approximation.

Mean wave drift loads are calculated for the fixed pontoons, therefore wave frequency motion effects are neglected. The reason is that the mean wave drift loads are calculated before solving the coupled motion responses by OrcaFlex,

Mean drift loads from waves are not included in the main load combination, as they were found to be of negligible value. It is included in the mooring analysis and in the direct simultaneous calculation of characteristic environmental loads.

Wave energy directional spreading is taken into consideration.

Wave-current interaction effects on the hydrodynamic loads is not taken into consideration.

Hydrodynamic interaction effects between pontoons is neglected.

Regarding current induced loads, although not described in the report, these are probably based on quadratic current coefficients. The source of the current coefficients is not referred.

5.3.3 Wind loads

Dynamic analyses of the straight bridge apply the nonlinear quasi-static airfoil theory (NQSA) described in 3.1.1. Aerodynamic coefficients for the girder were obtained through literature study, 3D RANS simulations, and 2D URANS simulations (Multiconsult, 2017c). The two CFD methods (considering three angles of attack) gave similar trends among different shapes, but significant differences were seen in the absolute reported values. Figure 24 and Table 9 from the Multiconsult report are reproduced here to illustrate the level of variation.

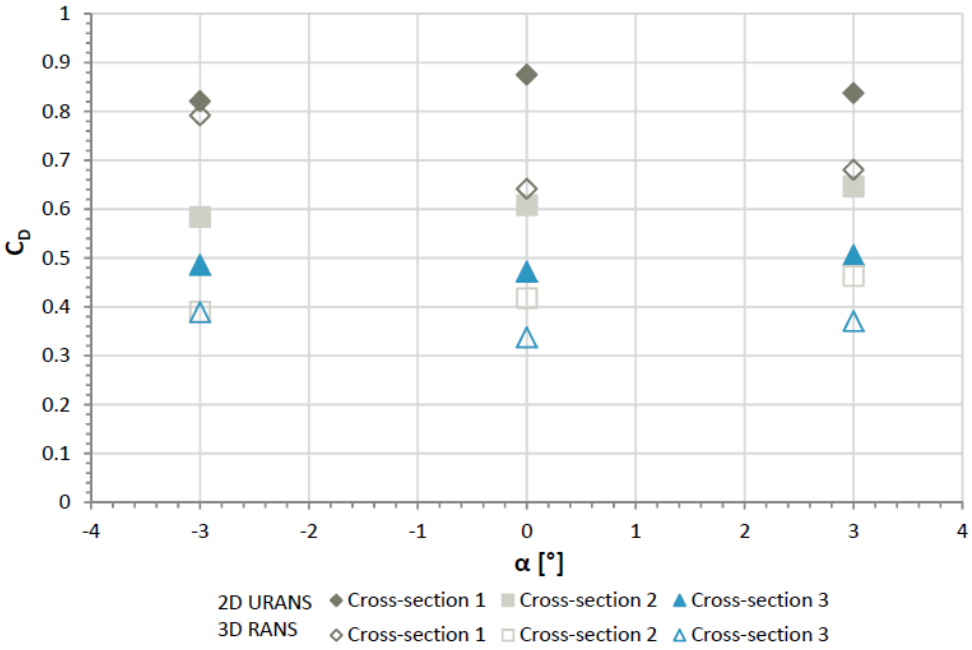

Figure 9: Figure 24 from (Multiconsult, 2017c) showing 3D RANS and 2D URANS results for the drag coefficient of three girder section designs.

Table 4: Table 9 from (Multiconsult, 2017c) showing 3D RANS and 2D URANS results for the lift and moment derivatives.

Cross section		3D RANS	2D URANS
1	C_L' [1/rad]	2.89	7.42
	C_M' [1/rad]	0.09	0.76
2	C_L' [1/rad]	5.33	5.38
	C_M' [1/rad]	1.39	1.27
3	C_L' [1/rad]	3.97	4.70
	C_M' [1/rad]	1.25	1.18

For the straight bridge tower sections, coefficients from literature were applied.

Flutter assessment for the straight bridge was carried out based on the eigenmode ratio and flat plate flutter derivatives.

5.3.4 Relevant observations

Some conclusions are relevant for understanding the effects of wave, wind and current load actions:

- The weak axis moment response is dominated by vertical and pendulum eigenmodes. The longest vertical eigen period in the low part of the floating bridge is at 6.3s and the shortest vertical eigen periods with displacement of pontoons is at 3.3s.
- The dynamic wind contributes to the girder strong axis moment in the long period range, namely 20-60 s.
- The dynamic wind response is generally smaller than the response from waves.

- The response for the strong axis moments in the bridge girder is significantly reduced by the damping of the mooring lines
- The weak axis moment is reduced by hydrodynamic damping of pontoons.

5.4 Norconsult feasibility study

Norconsult carried out a feasibility study for the curved bridge solution (Norconsult, 2017).

5.4.1 Global Analysis

The methods for ULS global dynamic analysis are similar to those applied by Multiconsult and described in Section 5.3, but 3DFloat is used, instead of OrcaFlex. The coupled global dynamic loads and responses from waves/current and wind are calculated simultaneously by time domain 3DFloat for design conditions. Sofistik calculates linear static loads.

Fatigue analysis is performed by OrcaFlex and NovaFrame. Although detailed information was not found, OrcaFlex frequency domain solution is probably applied.

5.4.2 Wave and current loads

Wave/current and wind analyses for the design load cases are performed in the time domain with the 3DFloat software.

Current has not been included in the coupled analysis, but it is considered in the static solution by Sofistik.

The wave loads on the pontoons are calculated by Wadam in the frequency domain. Mean and slowly varying wave drift forces are also simulated based on Newman's approximation.

Slowly varying wave drift loads are not included in the coupled analysis. A simplified analysis showed that the strong axis peak moment increases with around 5% when wave drift forces are included.

5.4.3 Wind loads

Dynamic analyses of the curved bridge apply the nonlinear quasi-static airfoil theory (NQSA) described in 3.1.1. Aerodynamic coefficients for the girder were obtained through vortex simulations performed by COWI and by CFD simulations from IFE (again considering three angles of attack) (Norconsult, 2017). The results from different methods were again seen to differ significantly, with some simulations providing positive lift coefficients and other providing negative lift. The CFD studies investigated the effects of rails and the channelling effect of the sea surface, both of which were seen to influence all of the aerodynamic coefficients. Steady RANS simulations were found to underpredict the drag and overpredict the lift.

5.4.4 Relevant observations

Some observations related to the effects of wave, wind and current load actions include:

- Wind is the dominating load contribution for response about strong axis of the bridge. The strong axis response occurs mainly in the two first horizontal Eigen periods.
- Swell triggers horizontal modes in between 12 and 25s, but the contribution is minor compared to wind loading.
- Wind generated sea dominates the response about weak axis. A multitude of Eigen modes are triggered and the resonant behaviour is quite complex.
- Horizontal wave loading is a significant contributor to the dynamic response, inducing rotational deformation of the bridge girder. The structural response therefore depends on the height of the pontoon towers due to larger moment induced by the horizontal excitation force on the pontoons.

6. Identification of gaps

6.1 Wind loads

The choice of the "best" model for aerodynamic loads is not necessarily clear: NQSA maintains nonlinear terms, while FDAC captures frequency-dependent effects which are not present in NQSA. For large motions or extreme turbulence, NQSA may therefore better capture the real loads. For stability analysis, FDAC would be preferable. At the time of writing, the available aerodynamic coefficients for the Bjørnafjorden bridge designs are better suited to NQSA. FDAC coefficients may become available over the course of the project.

One may also consider extending the NQSA formulation to an unsteady airfoil formulation, for example following Beddoes-Leishman (Leishman & Beddoes, 1986), Theodorsen (Theodorsen, 1934) in frequency domain or Wagner in time domain (Peters, 2008), or Øye (Øye, 1991). The Øye model is already available in SIMA, although the built-in time lags may need re-visiting for bridge-type cross sections and the implementation would need to be enabled for sections which are not part of a wind turbine. This model would also require high-quality wind tunnel data as input. Such a model should be compared to other approaches using Volterra series or a rheological model (Carassale, 2014) (Diana G. R., 2006).

Other gaps related to the wind loads which arise due to the length of the bridge or due to the floating nature of the structure are more related to the wind field rather than the load models. The needed discretization in the wind field for a long floating bridge is not straightforward to define, and the implementation of a non-homogeneous mean wind speed may be practically challenging in some software (due to the frozen turbulence assumption). Similar practical challenges may arise for variable spectral density or coherence along the length of the bridge. The selection of relevant cases – relating the wind speed to the wave and current conditions – will also be a challenge. Given that one can obtain the incoming wind vector at different points along the bridge, however, the existing wind load models are anticipated to be sufficient.

6.2 Wave and current loads

Several gaps have been identified along the report on the state-of-the-art methods for calculation of wave and current loads on large floating bridges. These are related to specific characteristics of the structure, which are different from typical offshore problems, and not to different physics. This means that formulations developed and validated for offshore problems may be directly used for floating bridges. For most problems, but not all, the existing computer codes can be directly applied, or adapted. For most of the gaps identified, the challenges are related to adapting the existing methods to a very complex elastic structure. For most cases it does not mean that the tools are not able to cope with the problems (not the cases of inhomogeneity), but the numerical modelling is demanding and the computational effort unbearable. Simplifications are required; however the consequences of such simplifications have not been investigated.

The following sub-sections describe the identified gaps for wave and current loads.

6.2.1 Inhomogeneous wave and current loads

Calculation of inhomogeneous wave and current loads requires a consistent description of the environment along the bridge and the capability of the global analysis software to account for different environments along the bridge span. In between these two steps, one needs to calculate current and wave loads coefficients.

Calculation of current load coefficients for inhomogeneous currents is not seen as a problem (see 3.2.12).

On the other hand, calculation of wave load coefficients for inhomogeneous wave fields is more complex and there are limitations related to the use of FD diffraction codes, which solve the boundary value problem for ("homogeneous") harmonic waves:

(a) If the global analysis is performed in the frequency domain, then, in principle, the global analysis is connected to the diffraction solution, and the solution is obtained frequency by frequency for harmonic waves (as a consequence the wave filed is homogeneous).

(b) If the global analysis is performed in the time domain, then, depending on the actual software, it might be possible to consider different seastates for different pontoons in the global analysis. This solution is consistent if interaction effects between pontoons can be neglected.

(c) If the global analysis is performed in the time domain and interactions effects between pontoons are relevant, then solution (b) is inconsistent. The diffraction interaction effects between floaters inherently assumed "uniform" harmonic waves along the array of floaters. If interaction effects are relevant, they will be calculated for uniform waves.

Presently and in the foreseen future, solution (b) is, apparently, the only option to account for inhomogeneity of wave loads. Being inconsistent does not necessarily mean the results are un-acceptable in practice. But the approach needs validation.

6.2.2 Slowly varying wave drift forces

We identify several gaps related to calculation of wave drift forces for floating bridge design, namely:

Effect of WF motions on drift forces

Effect of neglecting wave frequency motions. Existing global analyses assume wave drift forces can be calculated for the restrained floaters, however, it is known that wave frequency motions may have a significant effect on the wave drift forces.

Newman's approximation vs full QTFs

The common approach for calculating wave drift forces in real seastates is to assume Newman's approximation is valid, instead of using full QTFs. Again, studies are missing to validate this assumption for typical floating bridge floaters.

Wave-current interactions

Wave-current interactions have an important effect on the wave drift forces (and lesser on the 1st order motions). Wave drift forces increase for waves and current in the same direction. In case a current is present, calculation of wave drift forces should include current effects. One possibility is to apply the Aranha's formula, but the Brard number needs to be check, since it is likely that wave-current conditions are outside the range of validity for floating bridges conditions. The other option is to apply wave-current potential flow codes to calculate the wave drift forces.

Wave drift damping

Horizontal low frequency motions of the bridge, at the longest natural periods, are lightly damped. These motions are induced by low frequency content on both the wind and the wave excitation. The LF motion amplitudes are governed by the amount of damping, therefore a good estimation is essential. The wave drift damping is usually not considered for the global bridge analysis, while it is expected to have a relevant contribution to the overall damping. As in the previous point, one possibility is to apply Aranha's formula, but the validity needs to be checked. Wave-current potential flow codes can also be applied.

Short crested seastates

Wave conditions in the fiords are typically characterized by short crested seastates and/or combined wind seastates and swells with different directions. Directionality can easily be taken into account for calculation of linear wave excitation and first order motion responses. The same cannot be said for the wave drift forces, where consistent calculations require a very large computational effort not compatible with the bridge design. On the other hand, accurate calculation of wave drift forces for directional seastates might have an influence on the bridge modes which are excited. Approximations can be used, but they have not been validated.

6.2.3 Multi-body interactions

Multi-body interactions between floaters have been neglected for floating bridge analyses by assuming the distance between floaters is large. Apparently, there are not enough studies to relate the accuracy of this

approximation with the dimensions of the floaters and distance between floaters. However, it is known that hydrodynamic interactions may have a significant effect on the first order and second order responses.

6.2.4 Viscous damping effects

Viscous effects on the floaters may contribute to the wave frequency overall damping and/or to the wave excitation. The relative importance increases with the motion amplitude and with the frequency. Since incident waves and motion responses of floating bridge floaters are, in principle, of small amplitude, the relative importance of viscous effects is not obvious. Studies are needed to quantify this aspect.

Regarding viscous drift effects, these are expected to be small for floating bridges in conditions without current. For conditions with current, it might depend on the floater geometry and typical wave periods. Viscous drift may be present for floaters prone to separation with the current, if the wave periods are sufficiently long. These aspects require further investigation.

6.2.5 Shallow water effects

Finite water depth effects, including varying bathymetry, may have a significant influence on the wave loading, both first and second order. The actual relevance for floating bridges has not been assessed and it might be that such effects are not important, since floaters are used because the water depth is large. If finite water depth effects are relevant, it is possible to say that, for practical applications, finite water depth effects can be calculated with radiation/diffraction codes for horizontal sea bottoms only. Therefore, the following effects cannot be represented:

- Effects of the varying bathymetry on individual floaters.
- Effects of the varying bathymetry on multi-body interactions. Interactions between floaters are calculated either for a finite horizontal water depth, or for infinite water depth.

It is probably possible to apply approximations to achieve acceptable results, but studies on this topic are lacking.

7. Recommendations for further studies

The Section provides recommendations for further studies and developments to be carried out along the LFCS KPN project. These are related to the gaps identified in Section 6. It is recommended that all gaps are addressed during the project. However, for several of the gaps, only simplified studies, or discussions, are recommended, aiming at achieving a better understanding of the effects on the global analysis predictions. A few gaps are selected for more complete developments or studies.

Most of the proposed studies assume a functional SIMA/SIMO/RIFLEX numerical model for the case study floating bridge will be available.

Model test data is expected to provide important information, both for physical insight and for validation of numerical approaches. Ideally, the test program of WP5 should also take into consideration the studies recommended in this Section.

7.1 Wind loads

Two main activities related to wind load models are suggested:

1) Development of a SIMO-DLL for application of frequency-dependent wind loads. This approach will enable comparisons of the bridge responses considering the two most common wind load formulations. By applying the DLL approach, this will also serve as a pre-study to determine whether or not a more complete implementation should be pursued.
2) Simple comparisons of NSQA, FDAC, and nonlinear airfoil theory combined with dynamic stall could be carried out in order to determine whether or not dynamic stall models can be applied in order to model the most relevant effects. This approach would allow many existing wind turbine analysis tools to be applied more directly to floating bridge analysis.

7.2 Wave and current loads

Inhomogeneous wave and current loads

Effects of inhomogeneous wave and current loads on large floating bridges are considered important for the calculation of dynamic motion responses. This aspect will be further investigated along the FLCS project, both numerically and experimentally. SIMO and RIFLEX are the tools selected for the numerical analyses, with SIMA as the workbench. However, presently, SIMA/SIMO is not able to account for different environments for different pontoons. The limitation is related to simply handling of the input data.

The following tasks are proposed:

(a) Generalize SIMA/SIMO to handle different environments for different pontoons.

(b) Investigate the effects of neglecting wave inhomogeneity on the diffraction solution and propose approximations to deal with this limitation of existing panel codes. It is expected that the model tests will provide physical insight, as well as data to assess the effects and to validate the proposed approximation.

Investigation of the effects of different correlations of the wave field at the different pontoons is also considered important. This topic is not related to calculation of wave and current coefficients (WP2).

Multi-body interactions

Carry studies to assess the importance of multi-body hydrodynamic interactions between floaters on the WF responses and on the LF responses. Include systematic studies with varying distance between pontoons.

The multi-body hydrodynamic interaction model shall be validated by comparisons with model test data.

Viscous damping effects

Assessment of viscous effects generated at the floaters, on the WF and on the LF responses. Comparison of model test data with potential flow predictions will provide information on possible floater viscous effects. Applying viscous force coefficients in the global analysis numerical model will give the influence on the global responses.

Effect of WF motions on drift forces

Assessment of WF motions effects on the estimation of wave drift forces and on the global LF responses of the bridge. The method requires that the global solution is obtained on a first step, before the floater's WF motions are used in the estimation of wave drift forces, which then are applied for a second calculation of the global responses. In principle, one iteration is enough, if the coupling between the bridge LF and WF excited modes are weakly coupled.

Effect of wave-current interactions on wave drift forces

Assessment of wave-current interactions on the wave drift forces and on the LF bridge responses. Investigations shall include an evaluation of Aranha's formula by comparing with results from a wave-current panel code.

Model test data is important to provide evidence of possible effects on the LF bridge motions. It is also needed for validation of numerical approaches.

Wave drift damping

This study shall be performed in combination with the previous one (wave-current effects on drift forces). The methodology is the same.

Effect of short crested seastates on wave drift forces

Discussions on the effects of short crested vs long crested approach on the calculation of wave drift forces and on the bridge LF responses. Discussion on the application of superposition principle to calculate wave drift forces from wind waves and swell from different directions.

Newman's approximation vs full QTFs

Calculate and compare full QTFs with QTFs from Newman's approximation for one representative floater. Calculate and compare the drift force spectra for a range of representative seastates and assess the differences, especially for the frequency range covering the lowest bridge natural periods.

Shallow water effects

Discussions on the consequences of neglecting finite water depth effects on the calculation of WF and LF responses.

Discuss use of an approximation consisting of assuming horizontal bottom for one floater, or groups of floaters. In this case, effects of the varying bathymetry on multi-body hydrodynamic interactions is neglected.

8. References

AAS-Jakobsen. (2016). *Curved bridge - Navigation channel in south.*

AAS-Jakobsen. (2016). *Straight bridge, Navigation channel in south.*

Aas-Jakobsen, J. H. (2012). *Sognefjorden Feasibility Study of Floating Bridge.*

Agarwal, M. (2011). Incorporating irregular nonlinear waves in coupled simulation and reliability studies of offshore wind turbines. *Applied Ocean Research, 33*, 215–27.

Aranha, J. (1996). Second order horizontal steady forces and moment on a floating body with small forward speed. *J. Fluid Mech., 313*, 39-54.

Aranha, J. a. (1997). Slender body approximation for yaw velocity terms in the wave drift damping matrix. *Proceedings of 12th Int. Workshop on Water Waves and Floating Bodies.* Marseilles.

Bertram, V. (1990). Ship motions by a Rankine source method. *Ship Technology Reaearch, 37*, 143-152.

Bertram, V. (1998). Numerical Investigation of Steady Flow Effects in Three-Dimensional Seakeeping Computations. *Proceedings 22nd Symposium on Naval Hydrodynamics* (ss. 73-86). Washington, D.C.: National Academy Press.

Bertram, V. (2000). *Practical Ship Hydrodynamics.* Butterworth-Heinemann.

Carassale, L. W. (2014). Nonlinear Aerodynamic and Aeroelastic Analysis of Bridges: Frequency Domain Approach. *Journal of Engineering Mechanics, 140*(8).

Chen, X. (1994). Approximation on the quadratic transfer function of low-frequency loads. *BOSS ' 94, vol. 2.*, (ss. 289-302).

Chen, X. B. (1998). Interaction effects of local steady flow on wave diffraction-radiation at low forward speed. *Int. Journal of Offshore and Polar Engineering, 8(2)*, 102-109.

Cheng, Z. G. (2018). *Wave load effect analysis of a floating bridge in a fjord considering.* Engineering Structures, 197-214.

Cheng, Z., Gao, Z., & Moan, T. (2018). Wave load effect analysis of a floating bridge in a fjord considering. *Engineering Structures*, 197-214.

de Hauteclocque, G. R. (2012). Review of approximations to evaluate second-order low-frequency load. *International Conference on Offshore and Artic Engineering.* Rio de Janeiro.

Dev, A. a. (1994). Experimental evaluation of the viscous contribution to mean drift forces on vertical cylinders. *Proc. 7th Int. Conf. on the Behaviour of Offshore Structures (BOSS'94)* (ss. 855 - 875). Editor C. Chyssostomidis, Elsevier.

Diana, G. B. (1993). Turbulence effect on flutter velocity in long span suspended bridges. *Journal of Wind Engineering and Industrial Aerodynamics, 42*(2-3), 329-342.

Diana, G. R. (2006). A new numerical approach to reproduce bridge aerodynamic nonlinearities in time domain. *The Fourth International Symposium on Computational Wind Engineering.* Yokohama, Japan.

Faltinsen, O. M. (1974). Motions of large structures in waves at zero Froude number. *Proceedings of the International Symposium on Dynamics of Marine Vehicles and Structures in Waves* , (ss. 91–106). London.

Faltinsen, O. M. (1990). *Sea loads on ships and offshore structures.* Cambridge University Press.

Ferreira, M. a. (2009). Diffraction effects and ship motions on an artificial seabed. *24th International Workshop on Water Waves and Floating Bodies.* Zelenogorsk.

Fonseca, N. a. (2017). Wave drift forces and low frequency damping on the Exwave FPSO. *Proc. of the ASME 2017 36th Int. Conf. on Ocean, Offshore and Arctic Eng, June 25-30.* Trondheim.

Fonseca, N. a. (2017). Wave drift forces and low frequency damping on the Exwave Semi-submersible. *Proc. of the ASME 2017 36th Int. Conf. on Ocean, Offshore and Arctic Eng., June 25-30.* Trondheim.

Grue, J. a. (1993). The mean drift force and yaw moment on marine structures in waves and current. *J. Fluid Mech., 250*, 121-142.

Hermundstad, E. M. (2016). Effects of wave-current interaction on floating bodies. *Proc. 35nd Int. Conf. Ocean, Offshore and Arctic Engineering, OMAE2016, June 19-24.* Busan.

Hughes, G. (1954). Friction and form resistance in turbulent flow and a proposed formulation for use in model and ship correlation. *Transation of the Institution of Naval Architects, 96*.

Jain, A., Jones, N. P., & Scanlan, R. H. (1996). Coupled flutter and buffeting analysis of long-span bridges. *Journal of Structural Engineering, 122*(7), 716-725.

Kim, Y. a. (1998). A finite-depth unified theory for linear and second-order problem of slender ships. *Journal of Ship Research*, 51-60.

Lee, C. (2007). On the evaluation of quadratic forces on stationary bodies. *Journal of Engineering Mathematics 58*, 141-148.

Lee, C. H. (2004). Computation of wave effects using the panel method. I S. Chakrabarti, *Numerical Models in Fluid–Structure Interaction.* Southampton: WIT Press.

Lee, C.-H. (1995). *WAMIT Theory Manual.* MIT Report 95-2, Dept. of Ocean Eng. , MIT.

Lee, C.-H. a. (1989). Removind the irregular frequencies from integral equations in wave-body interactions. *Journal of Fluid Mechanics, Vol. 207*, 393-418.

Lee, C.-H. M. (1997). Computationas of wave loads using a B-spline panel method. *Proc. of 21st Symp. on Naval Hydrodynamics. Trondheim, Norway.* Trondheim.

Leishman, J. G., & Beddoes, T. (1986). A Generalized Model for Airfoil Unsteady Aerodynamic Behavior and Dynamic Stall Using the Indicial Method. *Proceedings of the 42nd Annual Forum of the American Helicopter Society.* Washington D.C. .

Multiconsult. (2017). *Bjørnafjorden, straight floating bridge phase 3. Analysis and design (Base Case). Appendix N - Aerodynamics.*

Multiconsult. (2017a). *Bjørnafjørden, straight floating bridge phase 3. Analysis and design (Base Case).*

Multiconsult. (2017b). *Bjørnafjørden, straight floating bridge phase 3. Analysis and design (Base Case). Appendix B - Environmental loads analysis.*

Multiconsult. (2017c). *Bjørnafjorden, straight floating bridge phase 3. Analysis and design (Base Case). Appendix N - Aerodynamics.*

Newman, C.-H. L. (2005). Computation Of Wave Effects Using The Panel Method. I S. Chakrabarti, *Numerical Models in Fluid-Structure Interaction.* WIT press.

Newman, J. (1974). Second order slowly varying forces on vessels in irregular waves. *Proceedings of the symposium on the dynamics of marine vehicles and structures in waves*, (ss. 182–6). London.

Norconsult. (2017). *K7 Bjørnafjorden end-anchored floating bridge. Global analyses summary.*

Norconsult. (2017). *K7 Bjørnafjørden End-anchored floating bridge. Summary report.*

Pessoa, J. a. (2013). Investigation of depth effects on the wave exciting low frequency drift forces by different approximation methods. *Applied Ocean Research*, 183-199.

Peters, D. (2008). Two-dimensional incompressible unsteady airfoil theory--An overview. *Journal of Fluids and Structures, 24*, 295-312.

Pinkster, J. (1980). *Low Frequency Second Order Wave Exciting Forces On Floating Structure.* PhD thesis.

Pinkster, J. V. (1977). Computation of the first and second order wave forces on oscillating bodies in regular waves. *Proceedings of the Second International Conference on Numerical Ship Hydrodynamics*, (ss. 1-21). Berkeley.

Rezend, F. L.-B. (2007). Second Order Loads on LNG Terminals in Multi-Directional Sea in Water of Finite Depth. *OMAE 2007.* San Diego.

Standard Norge. (2009). *Eurokode 1: Laster på konstruksjoner Del 1-4: Allmenne laster Vindlaster.* Standard Online AS.

Statens Vegvesen. (2015). *Bruprosjektering.* Hentet fra www.vegvesen.no

Statens Vegvesen. (2017). *Design Basis Bjørnafjorden Side- and end anchored floating bridge.*

Strømmen, E. N. (2006). *Theory of Bridge Aerodynamics.* Berlin: Springer-Verlag.

Theodorsen, T. (1934). *General theory of aerodynamic instability and the mechanism of flutter.* NACA.

Xu, Y., Øiseth, O., & Moan, T. (2018). Time domain simulations of wind- and wave-induced load effects on a three-span suspension bridge with two floating pylons. *Marine Structures, 58*, 434-452.

Zhao, R. a. (1989). Interaction between current, wave and marine structures. *Proc. 5th Int. Conf. on Numerical Hydrodynamics.* Hiroshima.

Zhao, R. F. (1988). Wave-current interaction effects on large volume structures. *Proc. Int. Conf. Behavior of Offshore Structures, BOSS 88* (ss. 623-638). Trondheim: Tapir Publishers.

Øye, S. (1991). Dynamic stall, simulated as a time lag of separation. *Proceedings of the 4th IEA Symposium on the Aerodynamics of Wind Turbines.* Harwell, UK: Harwell Laboratory.